Multi-measurement Depth Inversion Centre (MDIC)

2D LAND JOINT INVERSION OF SEISMIC, MAGNETOTELLURIC AND GRAVITY FOR PRE-STACK DEPTH MIGRATION IMAGING

Nechako Basin, British Columbia
Lines 05, 10 and 15

<u>Final Report</u>

Prepared for:

Geoscience BC

by

WesternGeco MDIC
Via Clericetti 42/A
Milan 20133
Italy

Report date: 1 October 2010

Deliverable list

On DVD Support:

Line 05	*Filtered PSDM stack* *PSDM converted to time stack* *PSDM final velocity field*	*Line05_PSDM.sgy* *Line05_D2T_PSDM.sgy* *Line05_PSDM_VELOCITY.sgy*
Line 10	*Filtered PSDM stack* *PSDM converted to time stack* *PSDM final velocity field*	*Line10_PSDM.sgy* *Line10_D2T_PSDM.sgy* *Line10_PSDM_VELOCITY.sgy*
Line15	*Filtered PSDM stack* *PSDM converted to time stack* *PSDM final velocity field*	*Line15_PSDM.sgy* *Line15_D2T_PSDM.sgy* *Line15_PSDM_VELOCITY.sgy*
Final Report	*Final_Report_Geoscience_BC.pdf*	

Involved personnel

Maurizio Sfolciaghi

Data Processing Supervisor, WG-MDIC

msfolciaghi@milan.westerngeco.slb.com

Marco Mantovani

Leader Seismic Geophysicist, WG- MDIC

mmantovani@milan.westerngeco.slb.com

Massimo Clementi

Project Leader, WG- MDIC

mclementi@milan.westerngeco.slb.com

Table of Contents

Figures

Tables

SUMMARY

The depth processing was characterized by the application of a joint inversion workflow of seismic, gravity and magnetotelluric data consisting of the derivation of tomographic velocities (turning rays) for the shallow section, followed by an iterative loop of pre-stack depth migration and velocity updates in a layer-stripping fashion from top to bottom of the model.

The velocity update during the depth migration workflow relied on iterative geologic-consistent velocity scans residuals for the portions with low S/N ratio and Common Reflection Point (CRP) tomography in Joint Inversion with MT data. The selection of the appropriate velocity parameters was conditioned by a relative improvement of the stacking power on the seismic section other than the flattening of migrated events in the Common Image Gather panels (CIG). The combined depth migration workflow allowed the definition of good structural details.

Verification of the results was performed by converting the PSDM sections to time (time stretching) using the interval velocity field used for migration. The comparison shows an acceptable time matching relative to the time migrated section, confirming the robustness of the derived velocity fields.

1. INTRODUCTION

This report describes the analysis and processing applied to the Nechako Basin 2D data set. In particular Line 05, 10, and 15 were processed. The total length of processed lines was approximately 80 km.

The seismic dataset was acquired with Vibroseis sources in 2008. Figure 1 displays the survey area location and the localization of 2D lines.

The processing is aimed at defining better the regional structure of the basin which is largely covered by volcanics of variable thickness. The processing is based on a Joint Inversion technique using different geophysical domain such as seismic, gravity and magnetotelluric in order to obtain a better velocity model. The final purpose is to deliver a Pre-stack Depth Migration section and velocity model for each line.

The work was performed by *Westerngeco MDIC* for Geoscience BC, in WG's processing centre in Milan, Italy, from July 2010 to September 2010.

2. RECORDING PARAMETERS

The acquisition parameters may be summarized by the following table:

INSTRUMENTS	
RECORDING INSTRUMENTS	SERCEL 408XL
SERIAL NUMBER	15
SOFTWARE REVISION	8.1.35
VIBRATOR ELECTRONICS	PELTON ADVANCE II
DYN ACQUISITION SYSTEM	PELTON SHOT PRO
CAMERA MODEL	V12 PELTON
INSTRUMENT VALUES	
RECORD LENGHT	06 sec
LOW CUT FILTER	0
HI CUT FILTER	0.8 LINEAR PHASE
PRE-AMP GAIN	400 uV
NOISE EDITING	YES
SAMPLE RATE	2.0 ms
TAPE MODEL	LTO
TAPE DENSITY	100 gig
TAPE FORMAT	SEG-D IEEE
DIVERSITY STACK	ENABLED
SPREAD GEOMETRY	
DATA CHANNELS (ACTIVE PATCH)	960
ROLL IN/OUT	YES
PATCH SIZE	Push 720-pull240
AUXILIARY DESCRIPTIONS	
AUXILIARRY CHANNEL 1	C.T.B.
AUXILIARRY CHANNEL 2	T.REF
AUXILIARRY CHANNEL 3	W.REF
INFORMATION	
FIRST FILE #	00003
FIRST TAPE #	00006
SOURCE ARRAYS	
SOURCE POINT INTERVAL	40 m
SOURCE LINE ORIENTATION	SOUTH TO NORTH
RECEIVER ARRAYS	
RECEIVER POINT INTERVAL	20 m
RECEIVER LINE ORIENTATION	SOUTH TO NORTH

VIBE SOURCE	
VIBE MODEL A	MERTZHD1 8 TRUCK
MODEL 1 HOLD DOWN (lbs)	52800 lbs
MODEL 1 DRIVE LEVEL (%)	080%
VIBE STATIC ARRAY	30 m
VIBE MOVE -UP	10 M
TOTAL DRAG LENGTH	60 M
VIBE GROUPING	1X4 INLINE
NUMBER OF VIBES	4
START FREQUENCY	8 Hz
END FREQUENCY	64 Hz
START TAPER	0.9 sec
END TAPER	0.9 sec
SWEEP LENGTH	28 sec
SWEEP TYPE	LINEAR
PHASE OFFSET	00 deg
NUMBER OF COMPOSITES	4
PILOT SWP TO G.F. RELATIONSHIP	180 deg
CHANNELS	
FIRST CHANNEL #	1
LAST CHANNEL #	960
GEOPHONE MODEL	
MANUFACTURER	SERCEL
MODEL	GS32CT
ORIENTATION	VERTICAL
COIL RESISTANCE	395 Ohms
SENSIVITY	0.7 v/in/sec
DAMPING	0.01%
PHONES PER SET	6
WIRING PATTERN	3x2
BASE TYPE	SPIKE
CONNECTOR TYPE	KCK
APPLICATION	LAND
SUB-SURFACE	NO
GEOPHONE ARRAY	
GEOPHONE SETS PER RECEIVER STN	1
GEOPHONE ARRAY LENGTH	20 m
INDIVIDUAL GEOPHONE INTERVAL	4 m

3. WIDE OFFSET PSDM

A wide offset depth migration (PSDM) was applied to processed line as described in Colombo (2005).

The PSDM processing used a datum plane of 1500 m above m.s.l. to which all depths are referred. The workflow used for the processing in depth is described below.

LINES 05, 10 AND 15: DEPTH PROCESSING RESULTS

An optimal processing sequence was defined for line 05, 10 and 15. The workflow used for the processing in depth is described in Appendix A.

Details on the processing tools applied are provided in the following paragraphs.

3.1.1. First break (FB) picking and initial model building

First break picking was provided by client on raw shot gathers (raw data) with a maximum picked offset of 3000 m. First-break quality (Figure 2) was acceptable for deriving the initial model for PSDM through turning ray tomography.

FB picking parameters:

Picked offset range: 0-3000 m

3.1.2. Gravity data

Processing of gravity data consists of calculating the Bouguer anomaly with the application of terrain correction.

It was used a Bouguer anomaly provided by Geoscience BC, calculated using a density of 2300 kg/m^3. The Bouguer anomaly was extracted from the starting 3D grid along each 2D line.

Gravity data were used jointly with first breaks picks in order to obtain a shallow velocity model from the topography to the maximum ray penetration.

3.1.3. Magnetotelluric data

Magnetotelluric data were provided by Geoscience BC along the 2D seismic profiles.

Resistivity model was used jointly with seismic residual moveout in order to obtain a deep velocity model.

3.1.4. Turning-ray tomography

The method applied for turning-ray tomography is a nonlinear inversion procedure, which adopts the finite-difference ray-tracing technique of Podvin and Lecomte (1991), the inversion algorithm LSQR of Paige and Saunders (1982) and the inversion scheme of Hole (1992). The tomographic procedure is able to handle sharp vertical and lateral velocity variations as well as sharp topographic changes.

The LSQR inversion provides a Conjugate Gradients solution to the system of equations obtained through linearization of the ray travel-time integral (by discarding all higher order terms of a Taylor expansion about a starting model). The solution is approached iteratively where the output of an inversion becomes the input of the successive inversion (non-linear inversion problem). The convergence to the final model is controlled by the decrease of r.m.s. residual versus the increase of model variance.

The linearization procedure transforms a non-linear inversion problem into an iterative solvable linear problem with the condition that the starting model of the inversion is a good guess of the actual velocity distribution. In this way the minimization of the travel-time residuals provided by the inversion procedure ensures that the solution converges to the global minimum of the objective function.

The starting model for the tomographic inversion was derived from the same FB data by using the refraction delay-time technique. Table 1 shows the performances obtained by turning-ray inversion.

3.1.5. Simultaneous Joint Inversion (JI)

The integration of seismic and non-seismic data has the purpose to improve velocity model building through integration of multiple geophysical domains. The goal is to evaluate quantitatively and probabilistically information from different geophysical sources such as seismic data, gravity data, electromagnetic data, structural interpretation and well information.

The joint inversion of seismic, gravity and magnetotelluric data solves the integration problem analytically. This approach is very different than simply converting parameters from one domain (e.g. seismic velocity) to another (e.g. density) and *vice-versa* using empirical functions (e.g. Gardner, 1974). The general formulation of the joint inverse problem follows the inverse theory from Tarantola (2003).

Because of the nature of the domains, Gravity data were jointly inverted with seismic refraction data (first breaks) in order to obtain the shallow model. Figure 5 display the resulting shallow velocity fields while Figure 8 Line 05: final shallow density model after JI with first breaks with the ray-coverage superimposed (blue line). Velocity scale is in Kg/m^3. show the final shallow density models.

Pre-Stack Depth Migration was run using the velocity model output from JI Gravity, and some interpreted layers were traced on the output seismic. From top to bottom, in a layer-stripping sense, seismic residual moveout along these layers were jointly-inverted with Magnetotelluric data to define the model for the deeper section.

The PSDM-Joint-Inversion workflow involving seismic travel-times, gravity and magnetotelluric data has been developed by Geosystem (Colombo and De Stefano, 2007) and successfully applied on Canadian foothills and thrust-belt seismic data in Oman (Colombo et al., 2007). Table 2 show respectively tomography and gravity performances in the JI process for modeling the shallow layers.

Table 1. Turning ray tomography performances.

Seismic line	Number of sources	Number of travel-times	Cell dimensions (m)	Initial r.m.s (ms)	Final r.m.s (ms)	Misfit improvement	Number of iterations
Line05	1060	333002	200x100	49.792	25.494	48.8%	5
Line10	970	291081	200x100	86.974	27.800	68.0%	6
Line15	378	101743	200x100	56.955	24.726	56.6%	5

Table 2. Gravity performances.

Seismic line	Number of gravity stations used	Density reduction (kg/m^3)	Initial r.m.s (mGal)	Final r.m.s (mGal)	Misfit improvement	Number of iterations
Line05	3622	2300	5.025	0.366	92.7%	5
Line10	1732	2300	5.725	0.239	95.8%	6
Line15	1356	2300	2.307	0.089	96.1%	5

Table 3 JI between MT and CIG residualsshows the information about the JI between MT and CIG residuals

Table 3 JI between MT and CIG residuals

Seismic line	Number of horizons	Total number of iterations
Line05	3	11
Line10	3	9
Line15	3	11

3.1.6. Wide offset PSDM (WOR-PSDM)

One advantage of wide offset PSDM is the ability to determine travel-time values for migration at all offsets and with any sharp velocity function (i.e. velocity changes in the order of 1:2). The most suitable method for deriving travel-time tables for long-offset data is the finite difference travel-time calculation obtained by solving the eikonal equation with the method of Podvin and Lecomte (1991), which is modified to avoid the generation of head waves at large offsets. Ray-tracing methods are also available for calculation of travel-times such as the maximum amplitude ray-tracing, where the amplitudes are accurately calculated and the travel-time with the maximum amplitude is used for duplicate arrivals, or the multi-arrival ray-tracing where up to five arrivals of significant energy are used to calculate the travel time table. These ray-tracing methods are indicated for complex velocity fields. The maximum amplitude ray-tracing approach was used for pre-stack depth migration.

Kirchhoff pre-stack depth migration allows the direct use of reflection tomographic methods (using ray-tracing) to perform the update of the velocity field within a migration velocity analysis procedure.

PSDM parameters:

Migration from topography

Type of algorithm: Kirchhoff

Travel time solver: maximum amplitude travel-time arrivals

Type: shortest-path

Depth interval: 10 m

Migration aperture: 3000 m (7000 m for 05)

Datum plane: 1500 m above m.s.l.

Maximum emergence angle: 45 degrees

Maximum frequency: 50 Hz

3.1.7. Migration velocity analysis (MVA)

Joint Inversion (JI) uses the depth residuals from both the common image gathers (CIG) and gravity field to derive updated interval velocity and density values.

For the velocity model building of line 05, 10 and 15, JI was performed iteratively. A new velocity model was generated after each JI iteration and if CIG data had to be used for the next iteration step, a new PSDM had to be performed. CIG residuals were evaluated for each PSDM-JI iteration.

The velocity model was sampled with a uniform rectangular mesh of 200mx100m along x and z directions respectively. On the other hand, the grid spacing for the density model increased away from the central region of interest (along both x and z). Furthermore the density model was extended laterally, relative to the velocity model, to take into account border effects.

Two Joint Inversion iterations were performed to refine the velocity model along geologically-consistent horizons. The velocity model building proceeded in a layer-stripping approach from top to bottom of the model. Interpretation and geological models provided by British Geological Survey were used as a reference for PSDM-JI processing. Figure 11 Line 05: initial velocity model superimposed on final PSDM stack (velocity scale in m/s). display the initial velocity models of depth processing after the shallow layers were solved while Figure 14 Line 05: final velocity model superimposed on final PSDM stack (velocity scale in m/s). show the final velocity model obtained at the end of the workflow. Figure 17 show the density model derived at the last joint inversion iteration. Figure 20, Figure 21 and

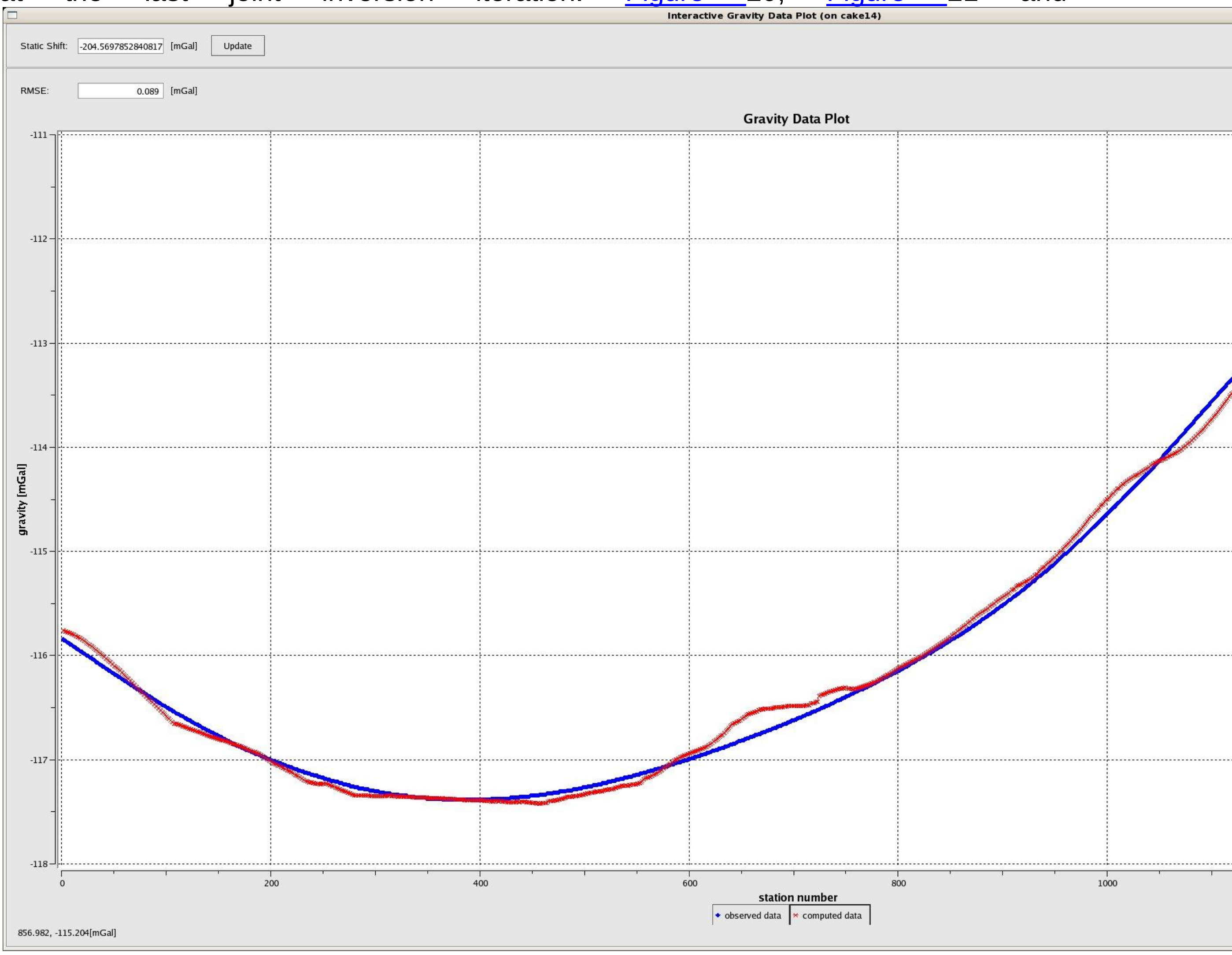

Figure 22 display the Bouguer anomaly fit of the last inverted model.

3.1.8. Bandpass Filter

A bandpass filter in depth domain was applied.

Bandpass Filter parameters:

Filter Frequency value: 3-5-28-36 Cycles/km at 1500 m

Filter Frequency value: 2-3-14-18 Cycles/km at 6000 m

3.1.9. Mute/Stack

Top and bottom mutes were manually picked along the lines in order to remove stretch effects and noise.

The traces within each cmp gather are stacked to form a single output trace. The resultant trace is the sum of the sample values normalized by the square of number of samples summed excluding hard zeroes.

3.1.10. Dip Scan Stack

A dip-scan stack technique was applied to enhance coherent seismic events in pre and post-stack domain.

This technique transforms the traces from t-x domain to a selected range of dip, or slant, stacked traces using a limited aperture Tau-P transform. Sample by sample, each dip trace is weighted by the semblance along that dip. The stronger, coherent events, independent of dip, have greater weights and contribute more to the inverse Tau-P transform which is then applied to back project to the t-x domain.

3.1.11. Automatic Gain Control

Automatic Gain Control (AGC) is applied to the data to bring up weak signal.

The AGC program moves the window down the trace sample-by-sample and calculates a scale factor at each location. The scale factor is equal to the inverse of the mean amplitude in the window. The scalar is applied to the sample at the centre of the AGC window.

3.1.12. Final Results

The final pre-stack depth migrated sections are displayed from Figure 23 to Figure 25 while Figure 26 to Figure 28 display the time-stretched version of the pre-stack depth migrated sections. The final PSDM velocity models are shown in Figure 29 Line 05: final velocity model..

The comparison of the time-stretched PSDM with the time migrated section indicates an overall similarity with respect to the absolute position in the time scale and to the geometry of the structures. Common image gathers (CIG) relative to the final migration are shown from Figure 32 to Figure 32. Where visible, the migrated events are flat at the various depths indicating correct migration velocities for all the offset components. For the portions of the model with poor S/N ratio, the criteria adopted for velocity updating was mainly based on the analysis of the stacking power subject to constraints deriving from the knowledge of the geology of the area.

4. CONCLUSIONS

The interval velocity field in depth for PSDM processing was derived by taking into consideration long-offset seismic phases such as wide-angle reflections and diving waves and a joint inversion scheme of seismic, gravity and magnetotelluric data that contributed to the definition of a robust velocity field for depth migration.

The Joint Inversion workflow shows various advantages over traditional approaches: the simultaneous use of different domains provides extended depth resolution relative to what can be achieved from the use of seismic data alone. In case of seismic data with poor S/N ratio, the gravity and MT contribution becomes important in the velocity determination problem.

A final comparison of the time-stretched PSDM section with the time migrated section and the analysis of the common image gathers suggest the overall correctness of the derived velocity field in depth domain. The depth migrated section shows enhanced definition of the complex structural setting.

5. REFERENCES

Colombo, D.	2005	Benefits of wide-offset seismic for commercial exploration targets and implications for data analysis, TLE, April 2005, 352-363.
Hole, J. A.	1992	Nonlinear high-resolution three-dimensional seismic travel-time tomography, J. Geophys. Res., 97, 6553-6562.
Colombo, D. and De Stefano, M.	2007	Geophysical modeling via simultaneous joint inversion of seismic, gravity, and electromagnetic data: Application to pre-stack depth imaging, TLE, March 2007, 326-331.
Gardner, G.H.F., Gardner, L.W., and Gregory, A.R.	1974	Formation velocity and density - the diagnostic basis of stratigraphic traps, Geophysics, 39, 770-780.
Colombo D., Mantovani M, De Stefano M., Garrad D., Hussain Al Lawati	2007	Simultaneous Joint Inversion of Seismic and Gravity data for long offset Pre-Stack Depth Migration in Northern Oman, 2007 CSPG Canadian SEG.
Paige, C. C. and M. A. Saunders	1982	LSQR: an algorithm for sparse linear equations and sparse least squares, ACM Trans. Math. Softw., 8, 43-71.
Simpson, R.W., Jachens, R.C., Blakely, R.J. and Saltus, R.W.	1986	A New Isostatic Residual Gravity Map of the Conterminous United States With a Discussion on the Significance of Isostatic Residual Anomalies. J. Geophys. Res., 91, No 138, 8348-8372.
Podvin, P. and I. Lecomte	1991	Finite difference computation of travel-times in very contrasted velocity models: a massively parallel approach and its associated tools, Geophys. J. Int., 105, 271-284.
Tarantola, A.	2003	Inverse problem theory: SIAM.

6. APPENDIX A

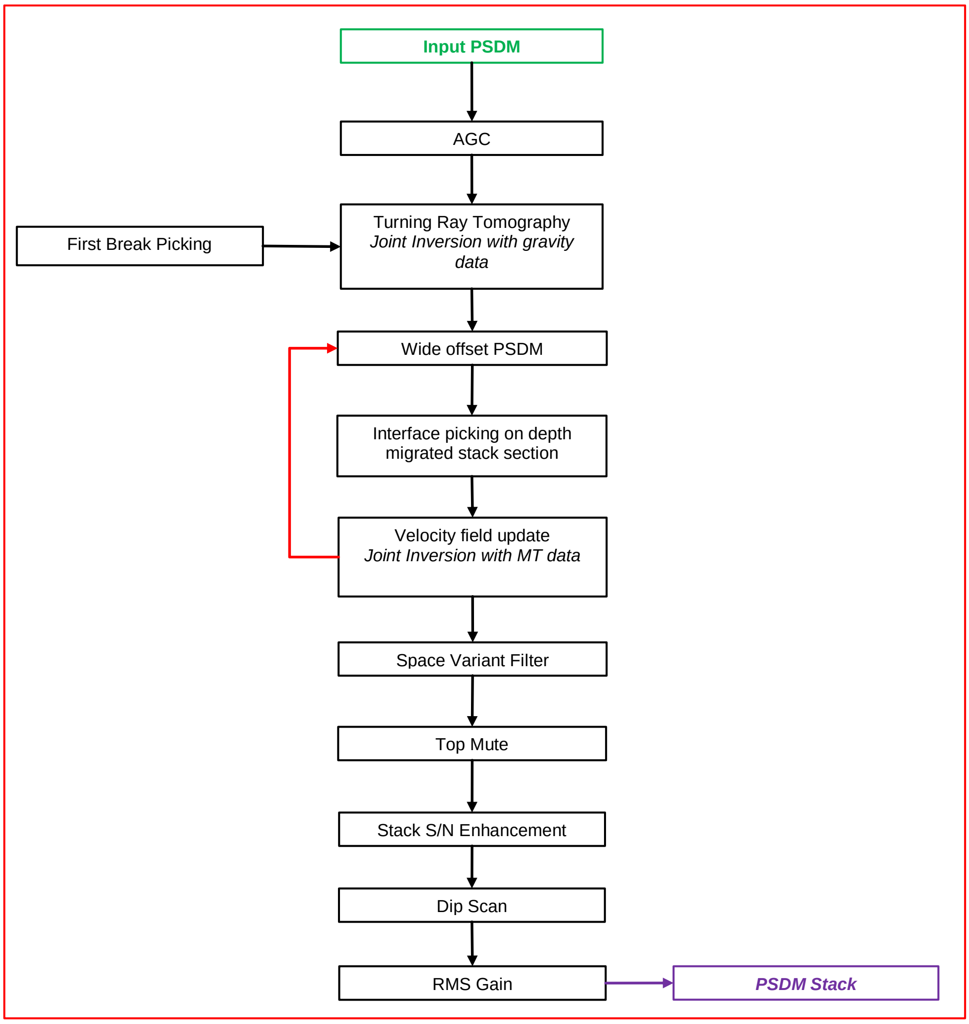
Input PSDM
AGC
First Break Picking
Turning Ray Tomography
Joint Inversion with gravity data
Wide offset PSDM
Interface picking on depth migrated stack section
Velocity field update
Joint Inversion with MT data
Space Variant Filter
Top Mute
Stack S/N Enhancement
Dip Scan
RMS Gain
PSDM Stack

7. FIGURES

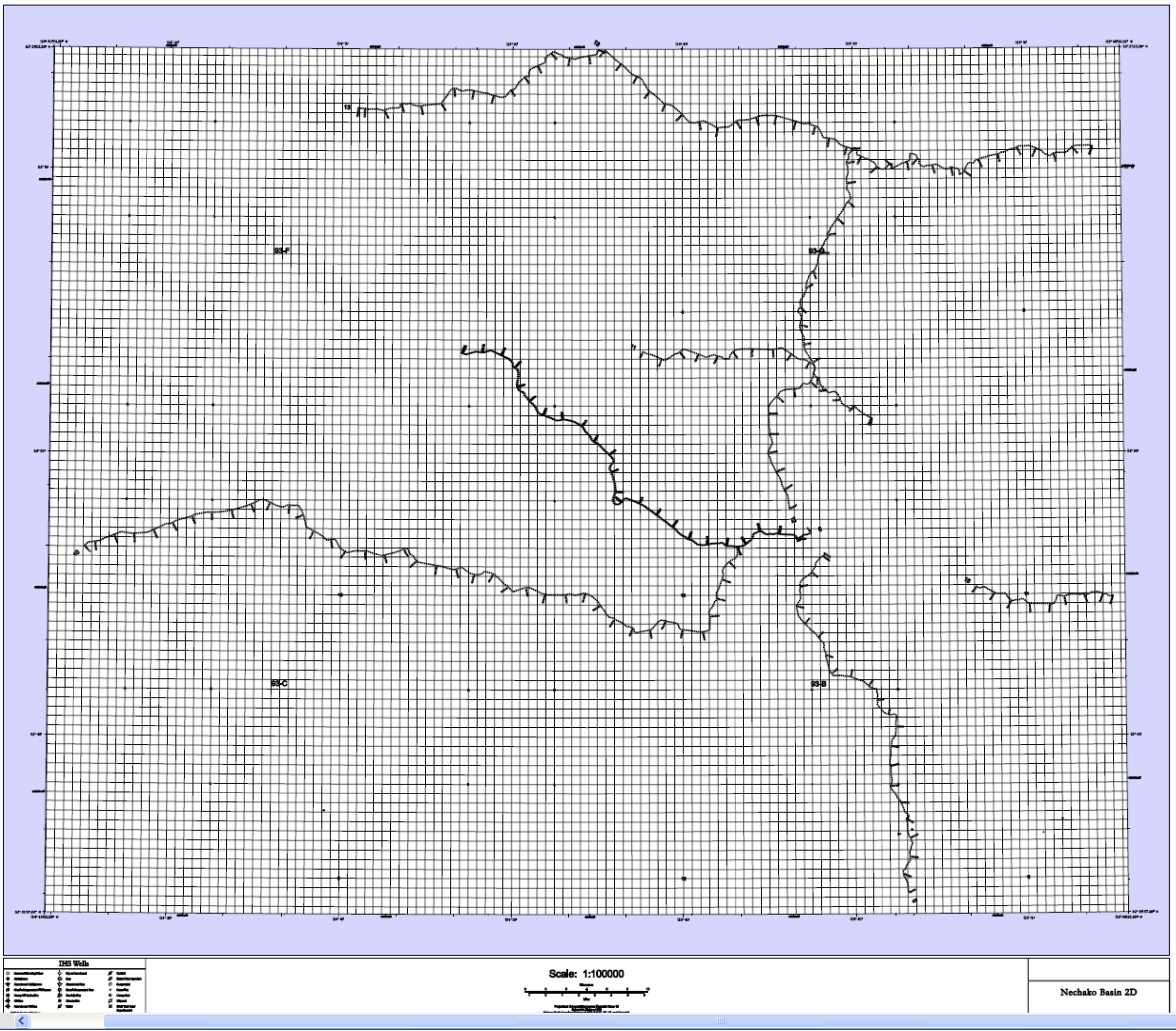

Figure 1. Survey area location.

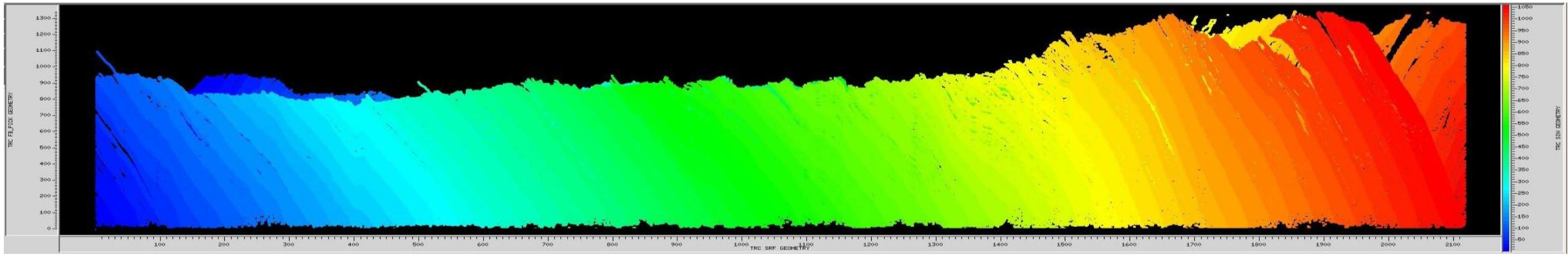

Figure 2 Line 05: First-break QC.

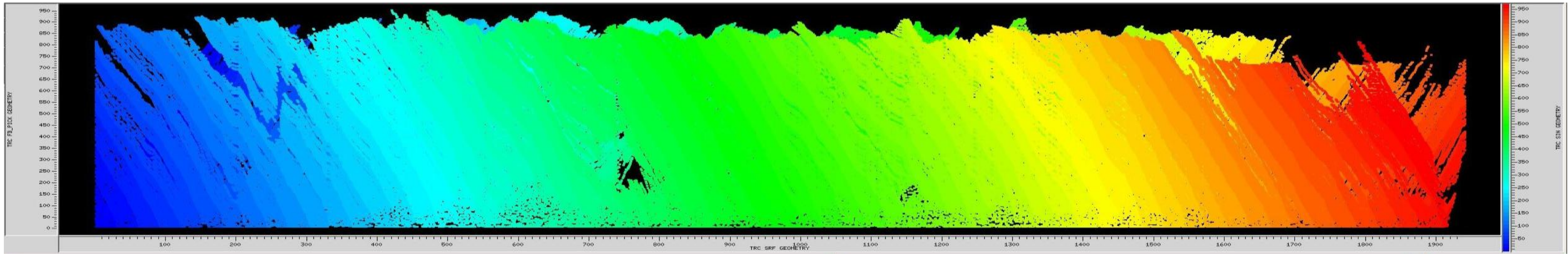

Figure 3 Line 10: First-break QC.

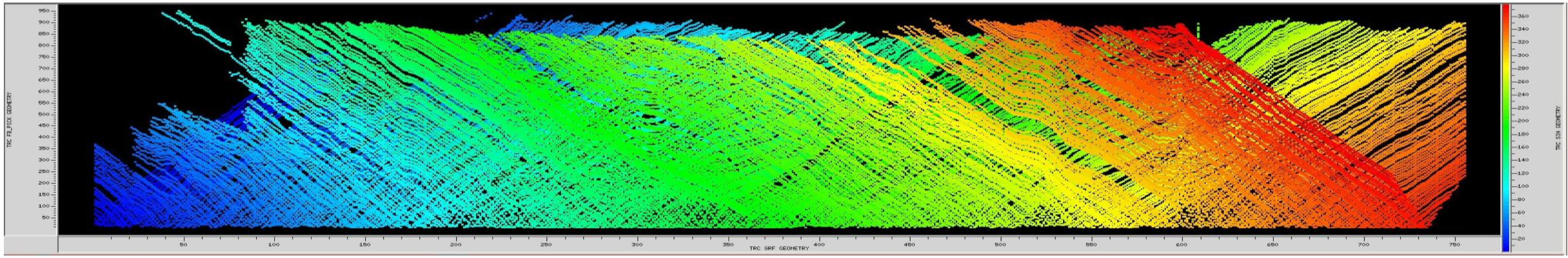

Figure 4 Line 15: First-break QC.

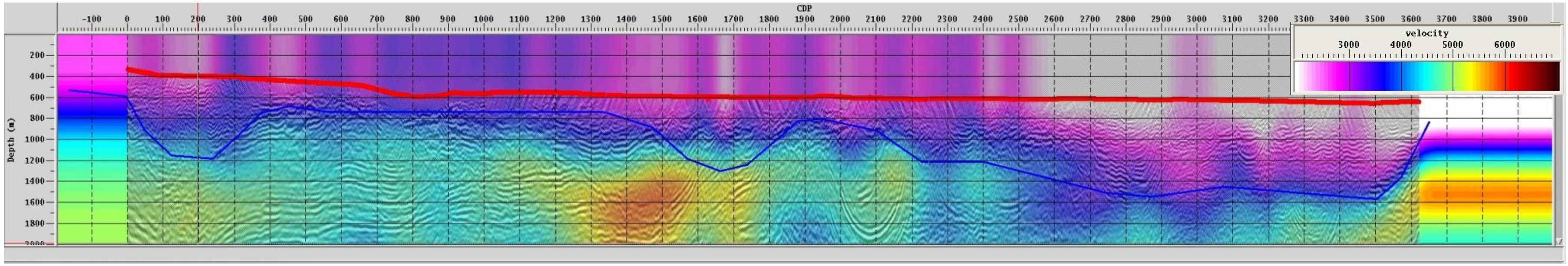

Figure 5 Line 05: final shallow velocity model after JI with first breaks and gravity with the ray-coverage superimposed (blue line). Velocity scale is in m/s.

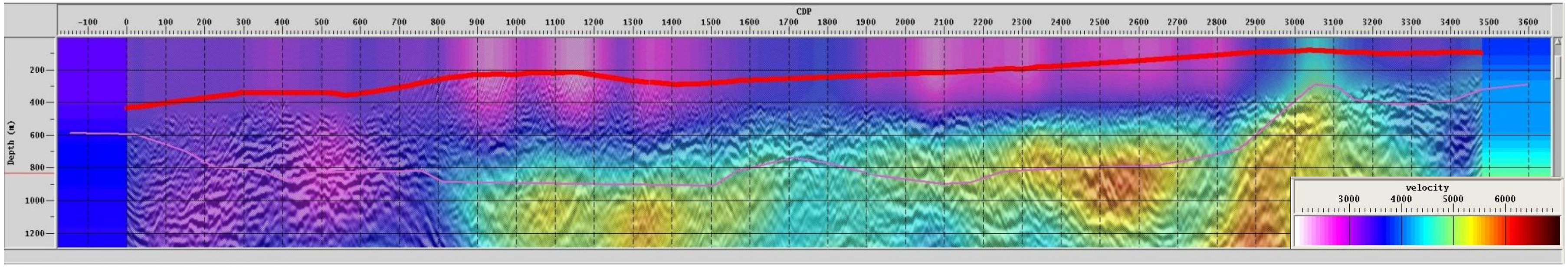

Figure 6 Line 10: final shallow velocity model after JI with first breaks and gravity with the ray-coverage superimposed (pink line). Velocity scale is in m/s.

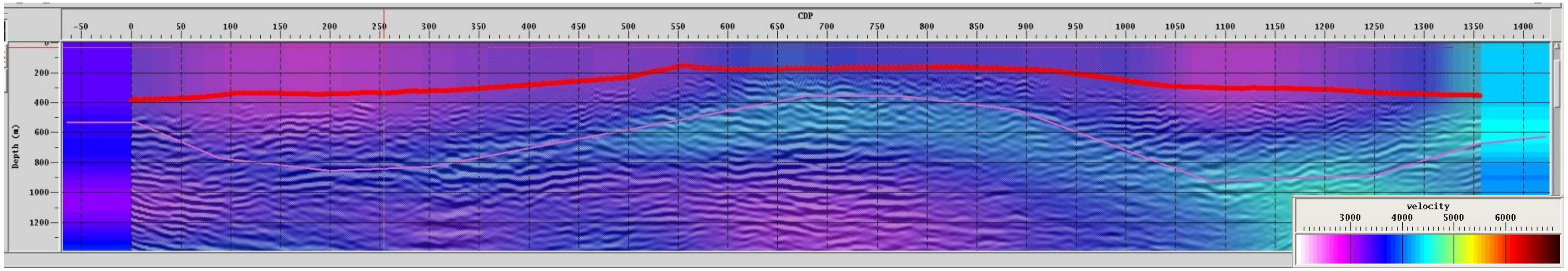

Figure 7 Line 15: final shallow velocity model after JI with first breaks and gravity with the ray-coverage superimposed (pink line). Velocity scale is in m/s.

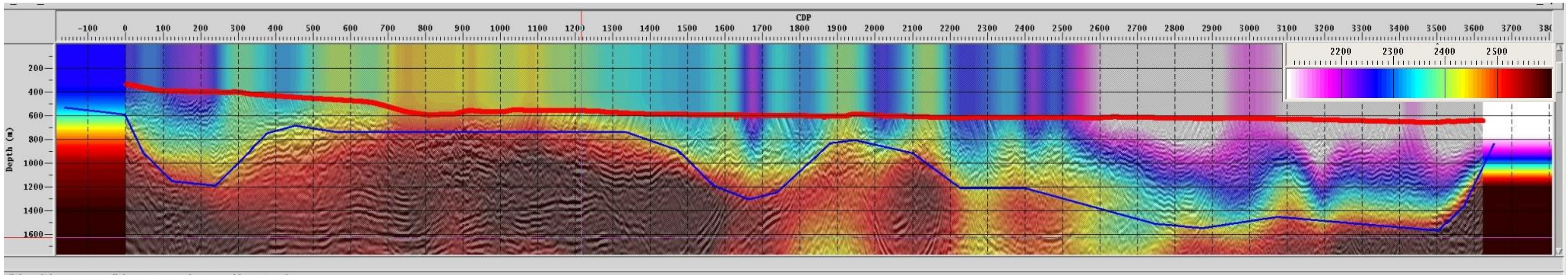

Figure 8 Line 05: final shallow density model after JI with first breaks with the ray-coverage superimposed (blue line). Velocity scale is in Kg/m^3.

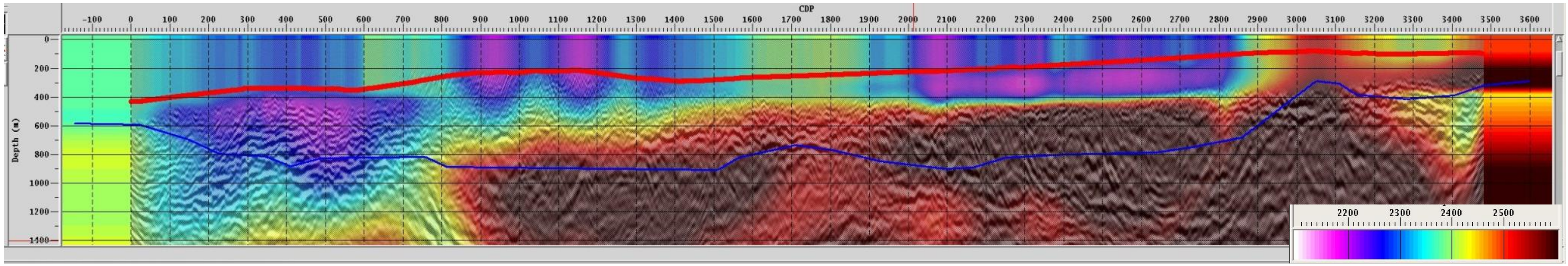

Figure 9 Line 10: final shallow density model after JI with first breaks with the ray-coverage superimposed (blue line). Velocity scale is in Kg/m^3.

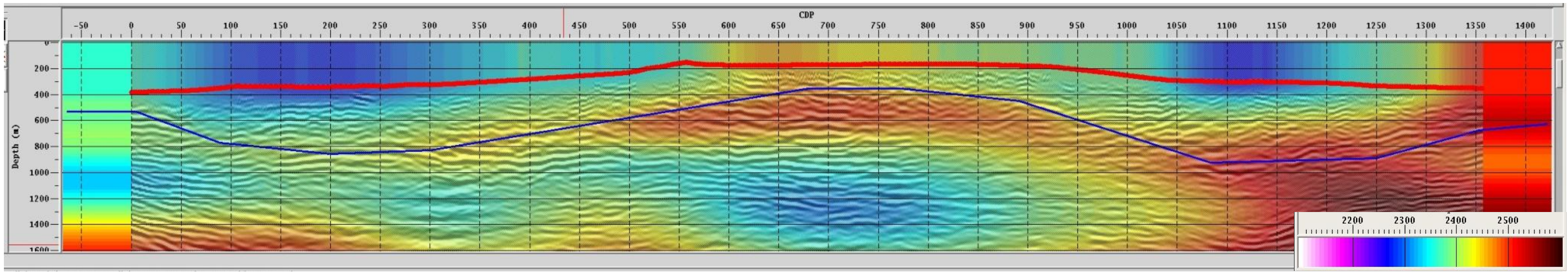

Figure 10 Line 15: final shallow density model after JI with first breaks with the ray-coverage superimposed (blue line). Velocity scale is in Kg/m^3.

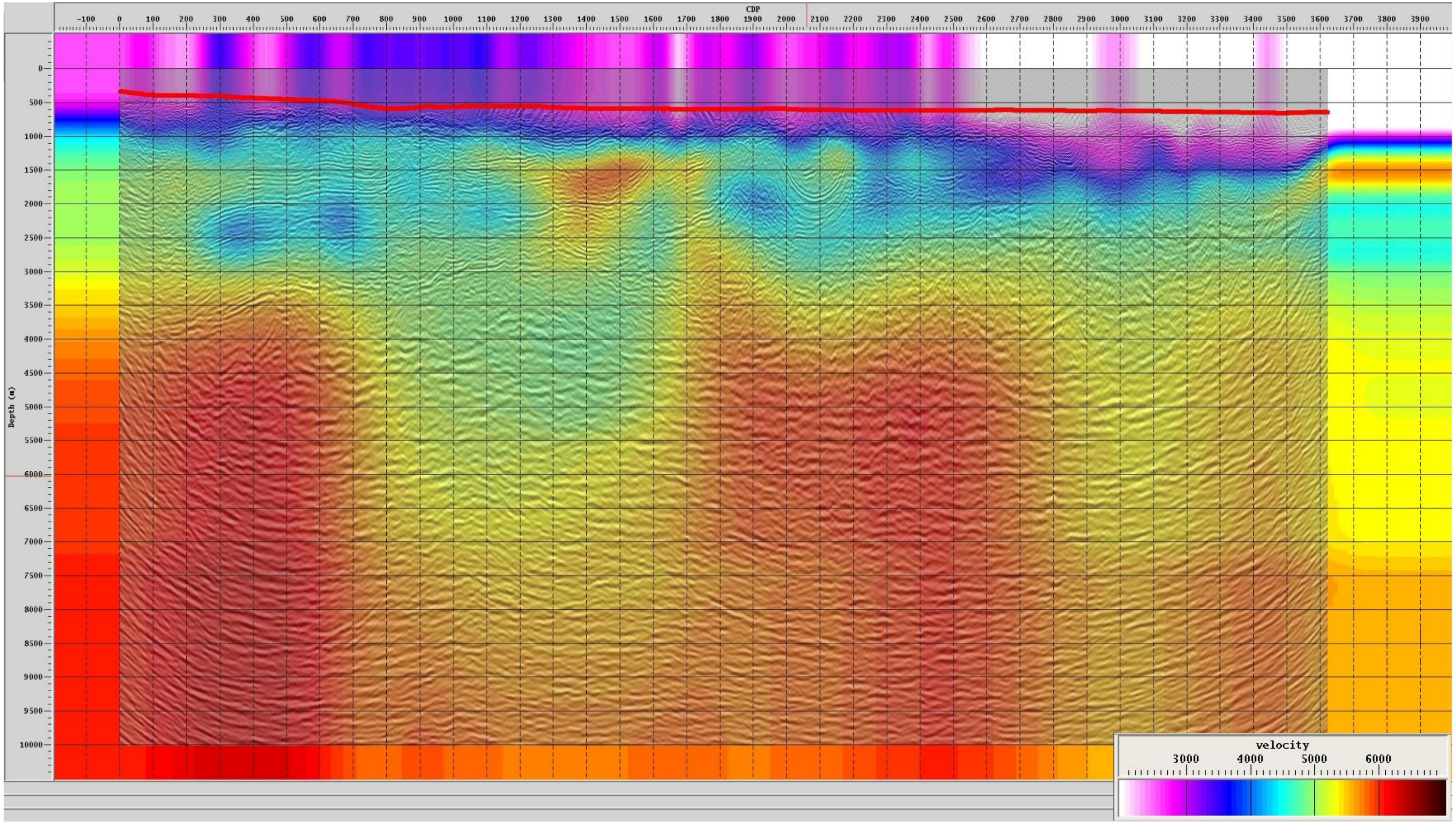

Figure 11 Line 05: initial velocity model superimposed on final PSDM stack (velocity scale in m/s).

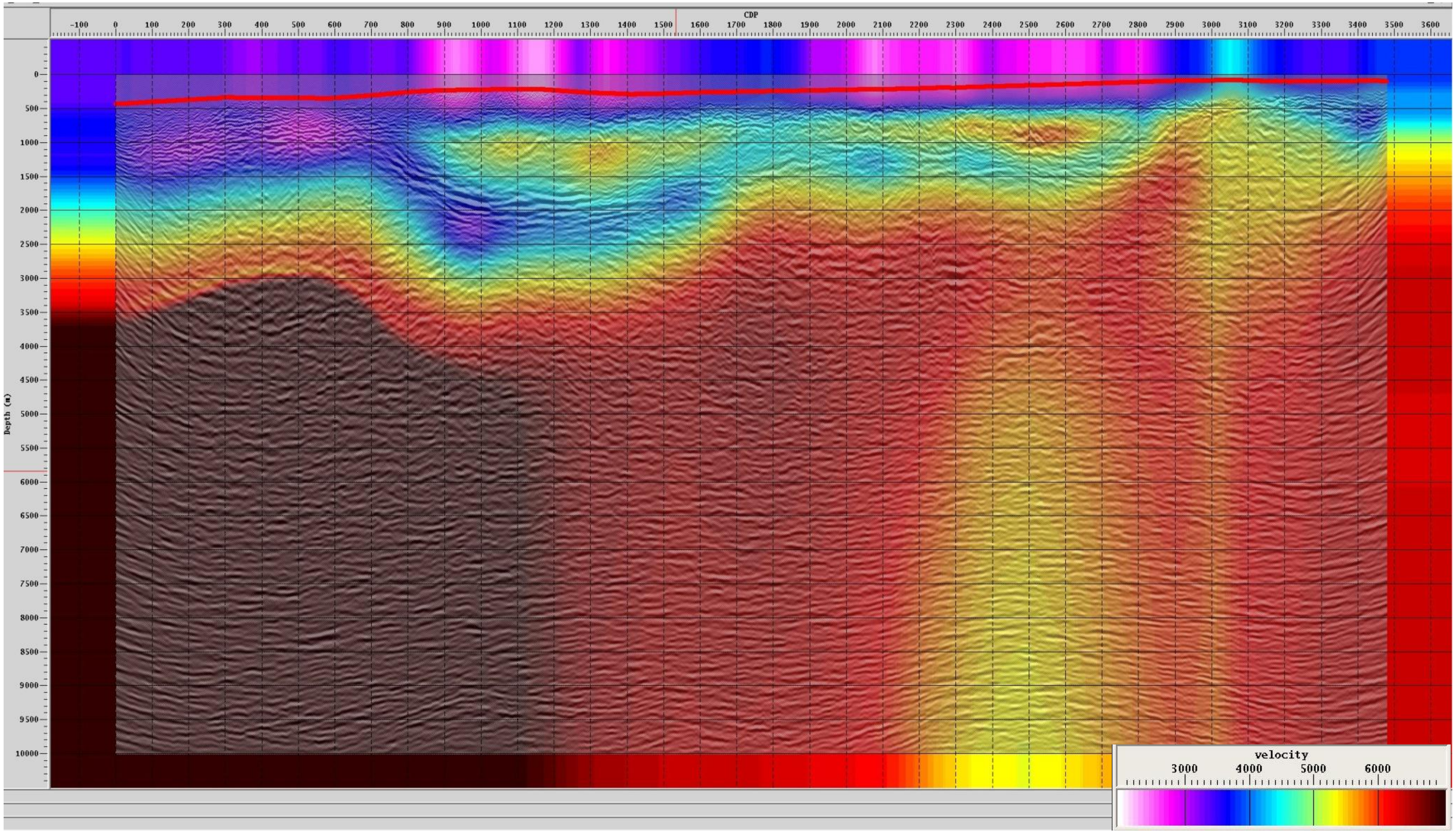

Figure 12 Line 10: initial velocity model superimposed on final PSDM stack (velocity scale in m/s).

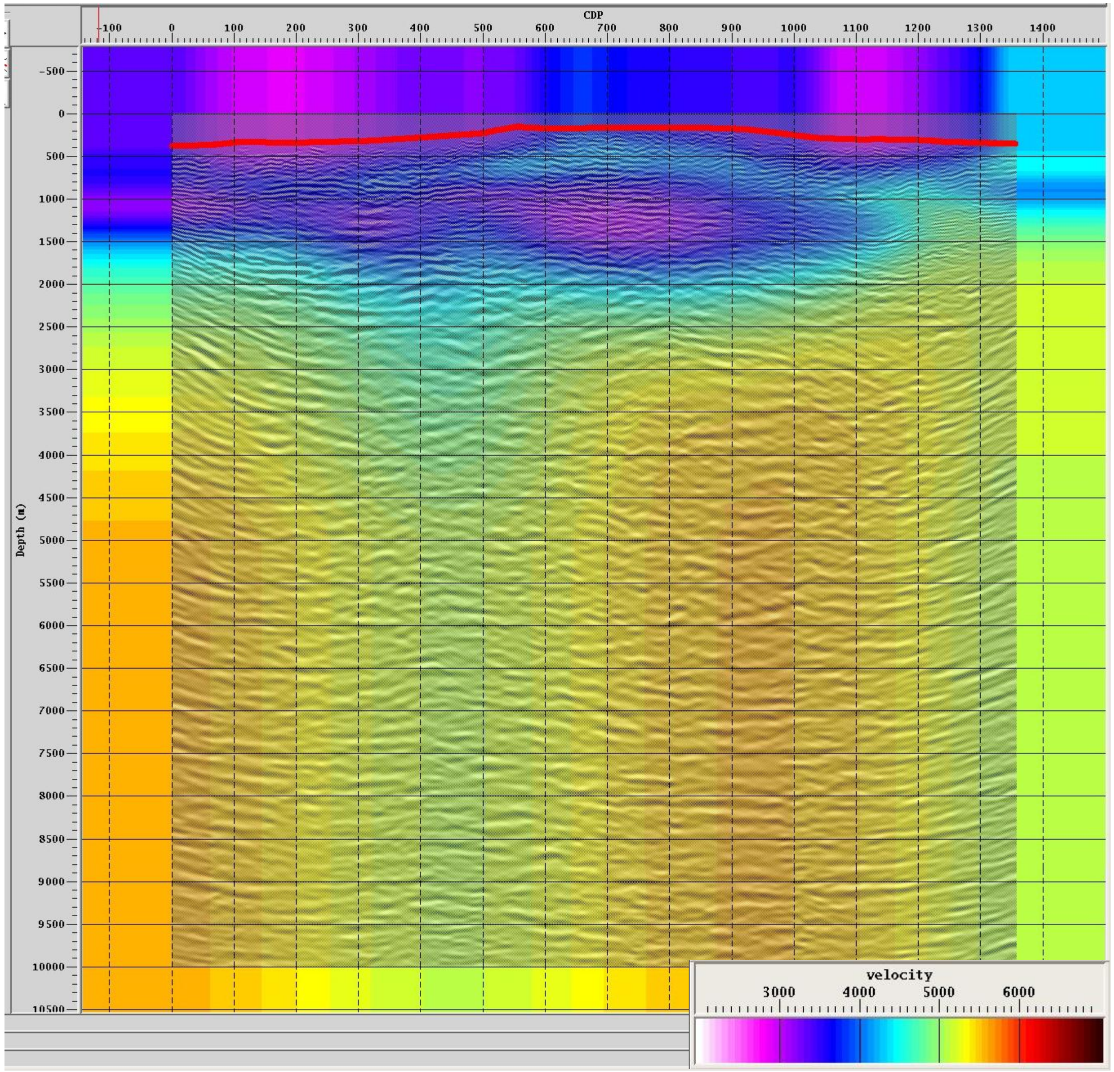

Figure 13 Line 15: initial velocity model superimposed on final PSDM stack (velocity scale in m/s).

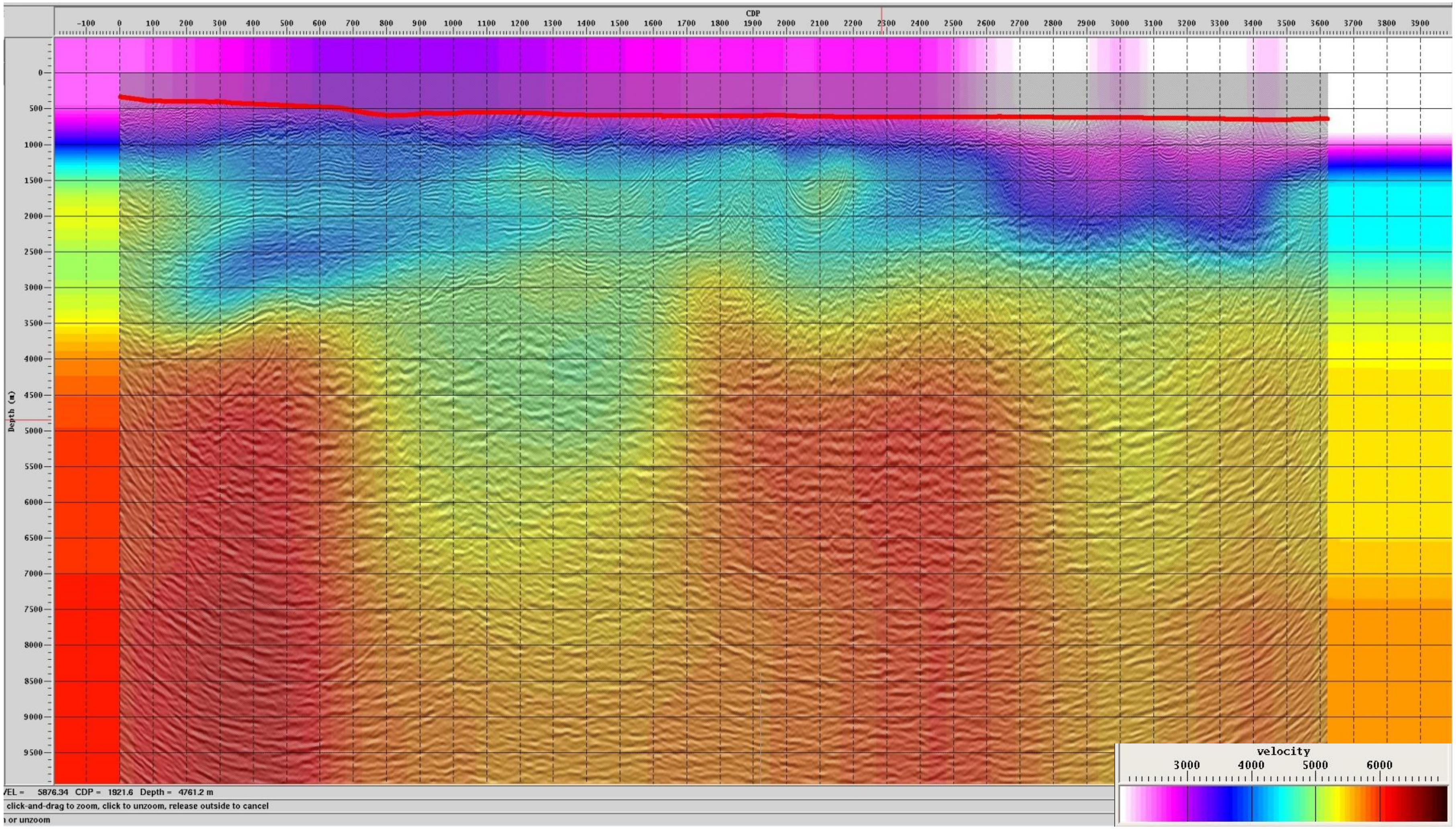

Figure 14 Line 05: final velocity model superimposed on final PSDM stack (velocity scale in m/s).

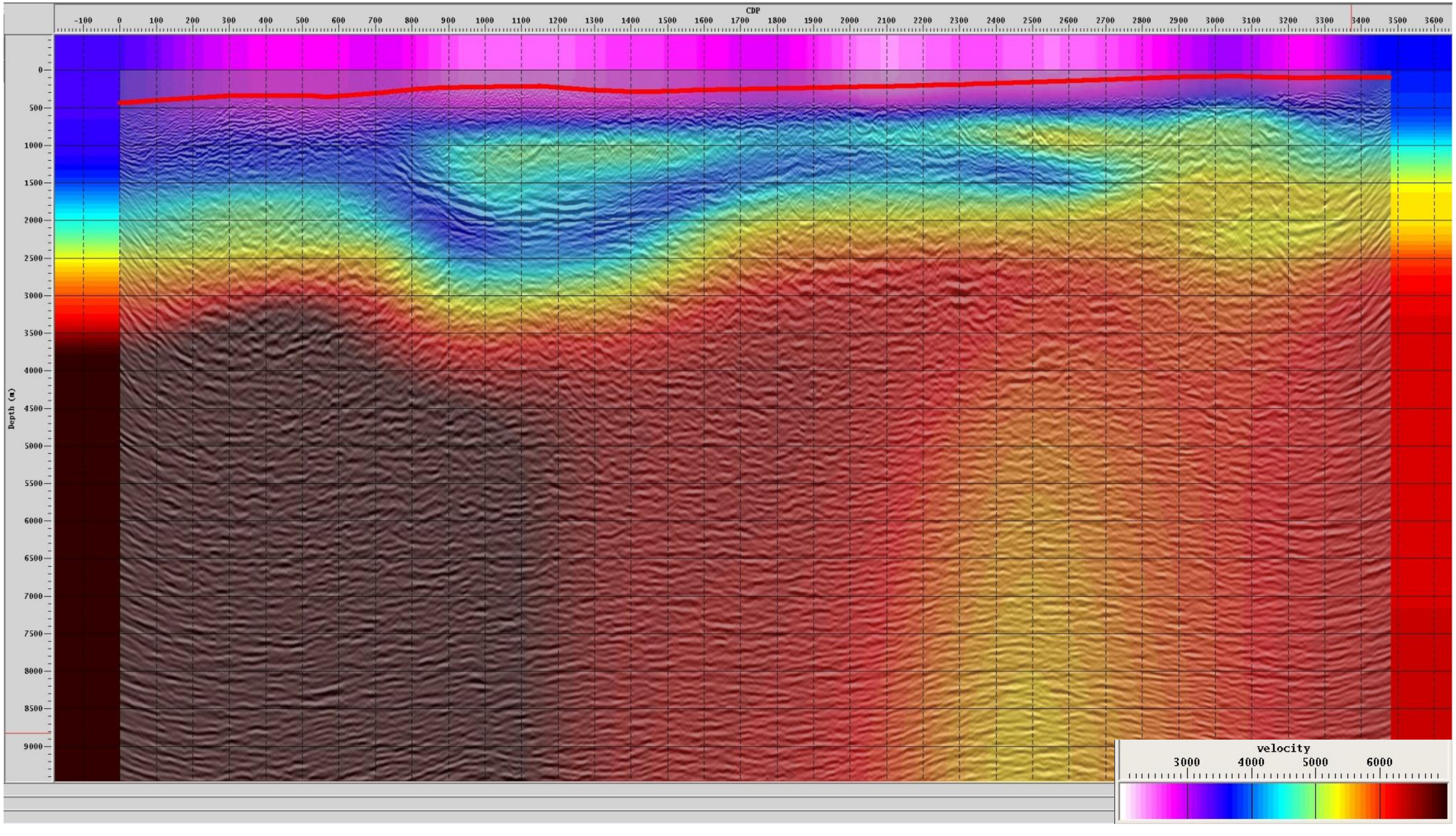

Figure 15 Line 10: final velocity model superimposed on final PSDM stack (velocity scale in m/s).

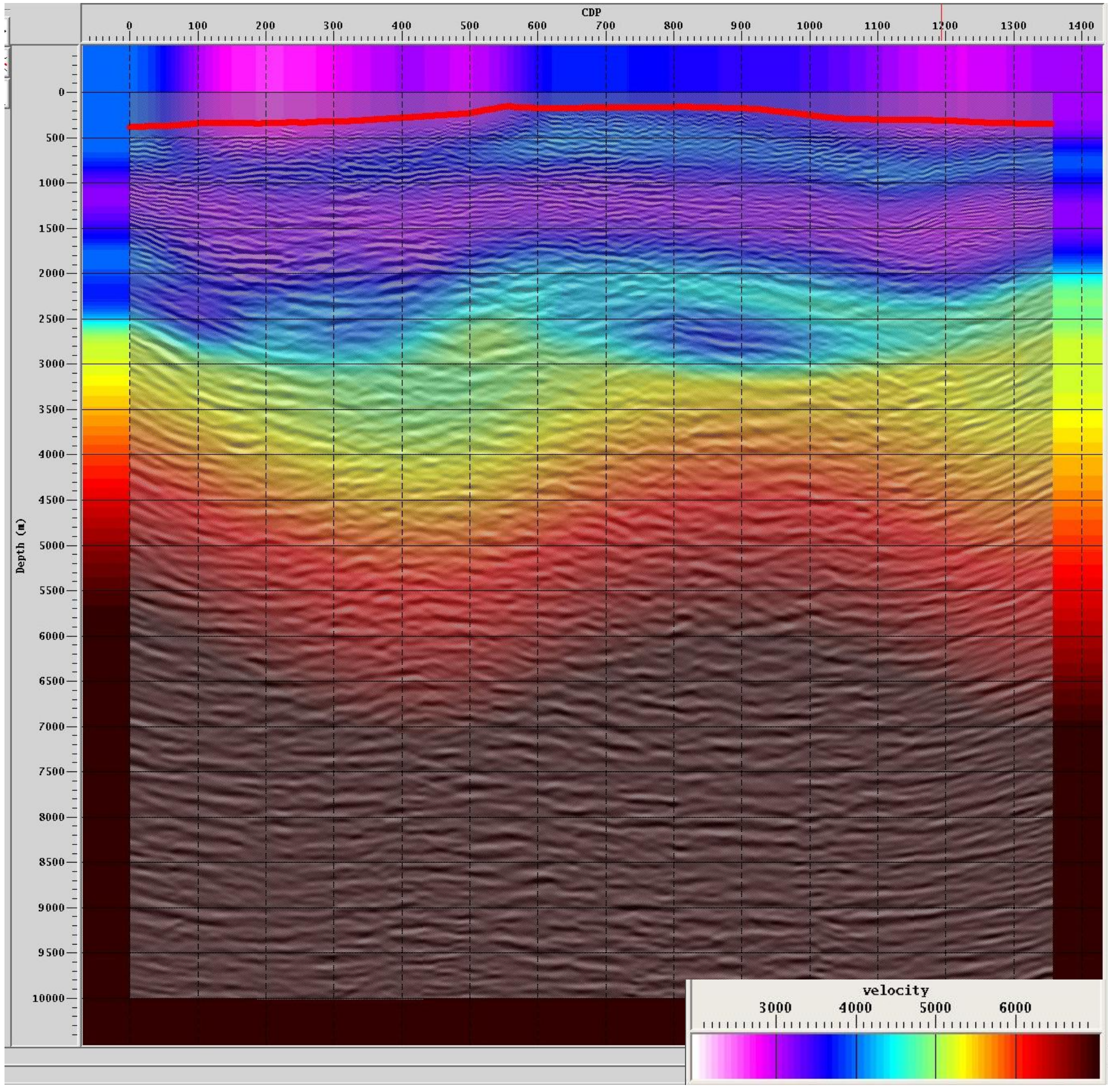

Figure 16 Line 15: final velocity model superimposed on final PSDM stack (velocity scale in m/s).

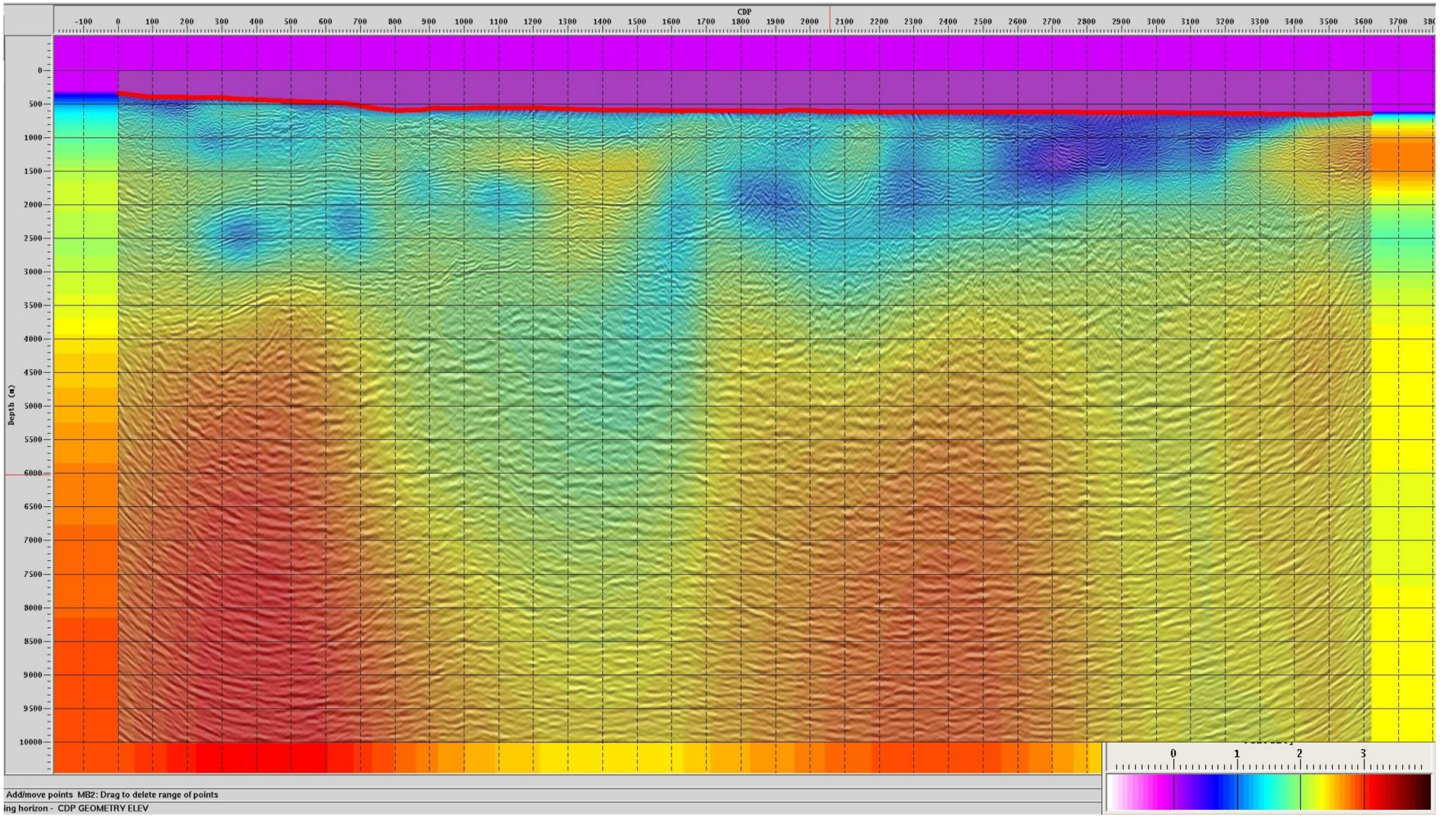

Figure 17 Line 05: final resistivity model superimposed on final PSDM stack, density scale in Log_{10}(kg/m3).

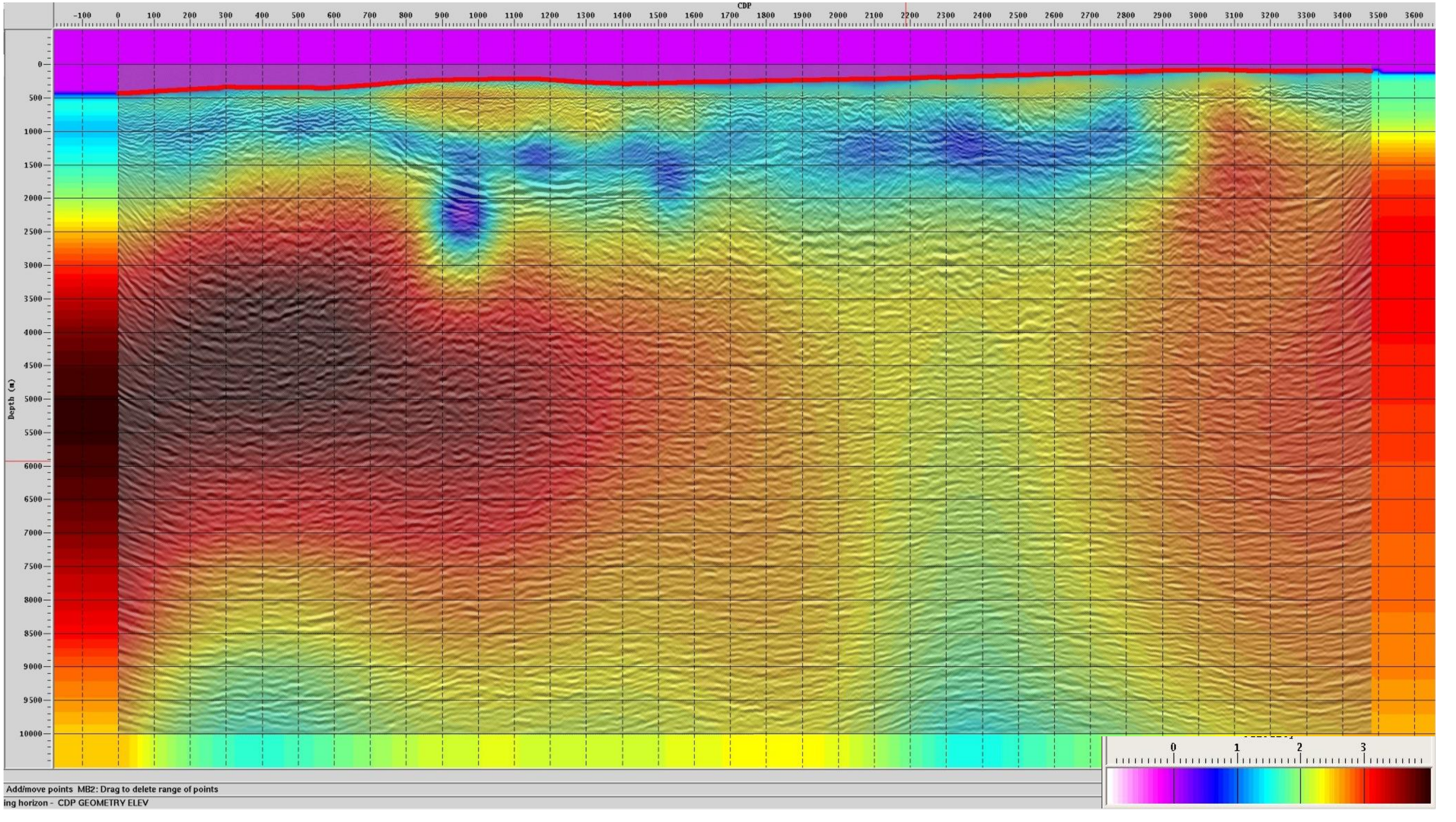

Figure 18 Line 10: final resistivity model superimposed on final PSDM stack, density scale in Log_{10}(kg/m3).

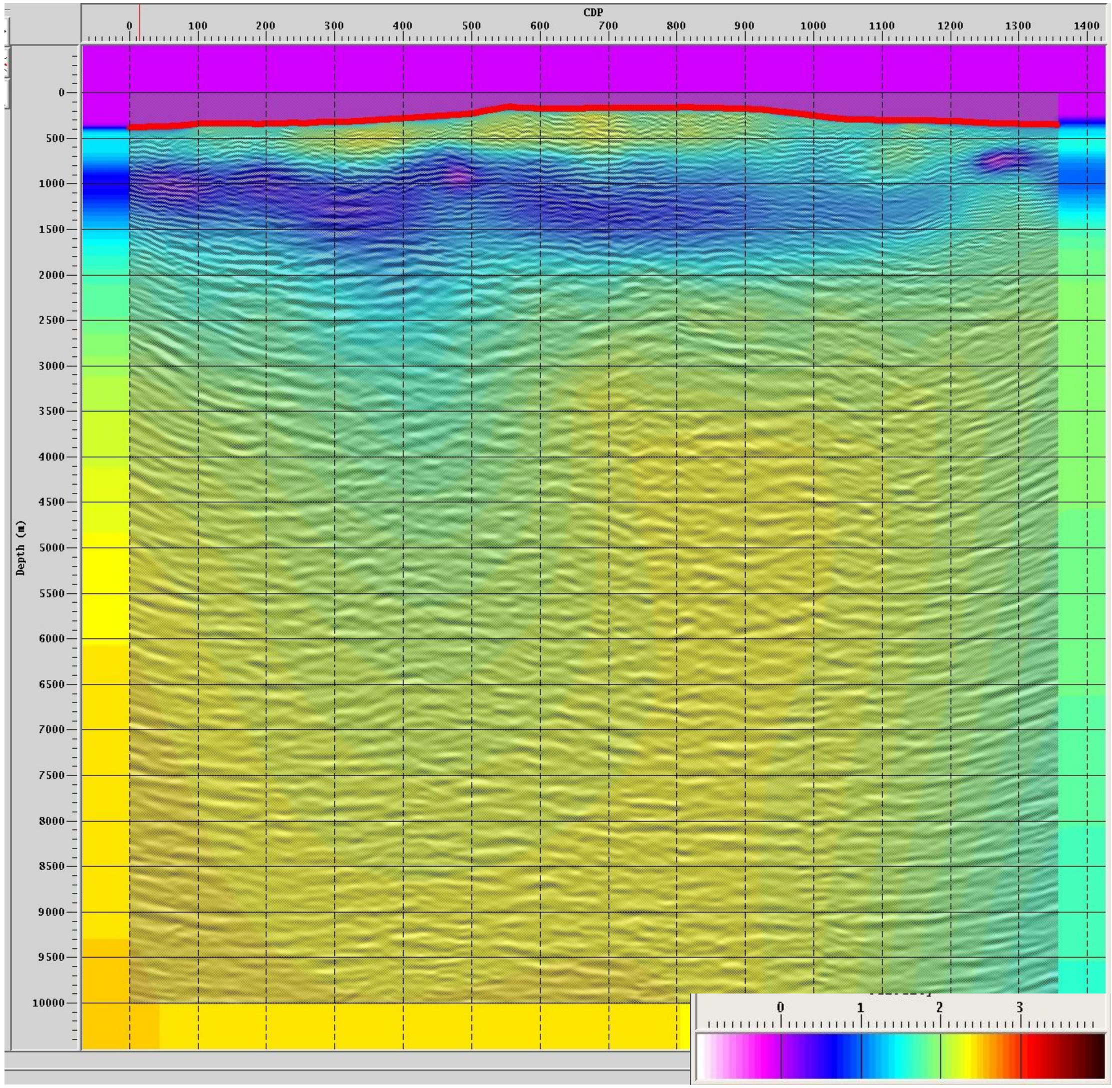

Figure 19 Line 15: final resistivity model superimposed on final PSDM stack, density scale in Log_{10}(kg/m3).

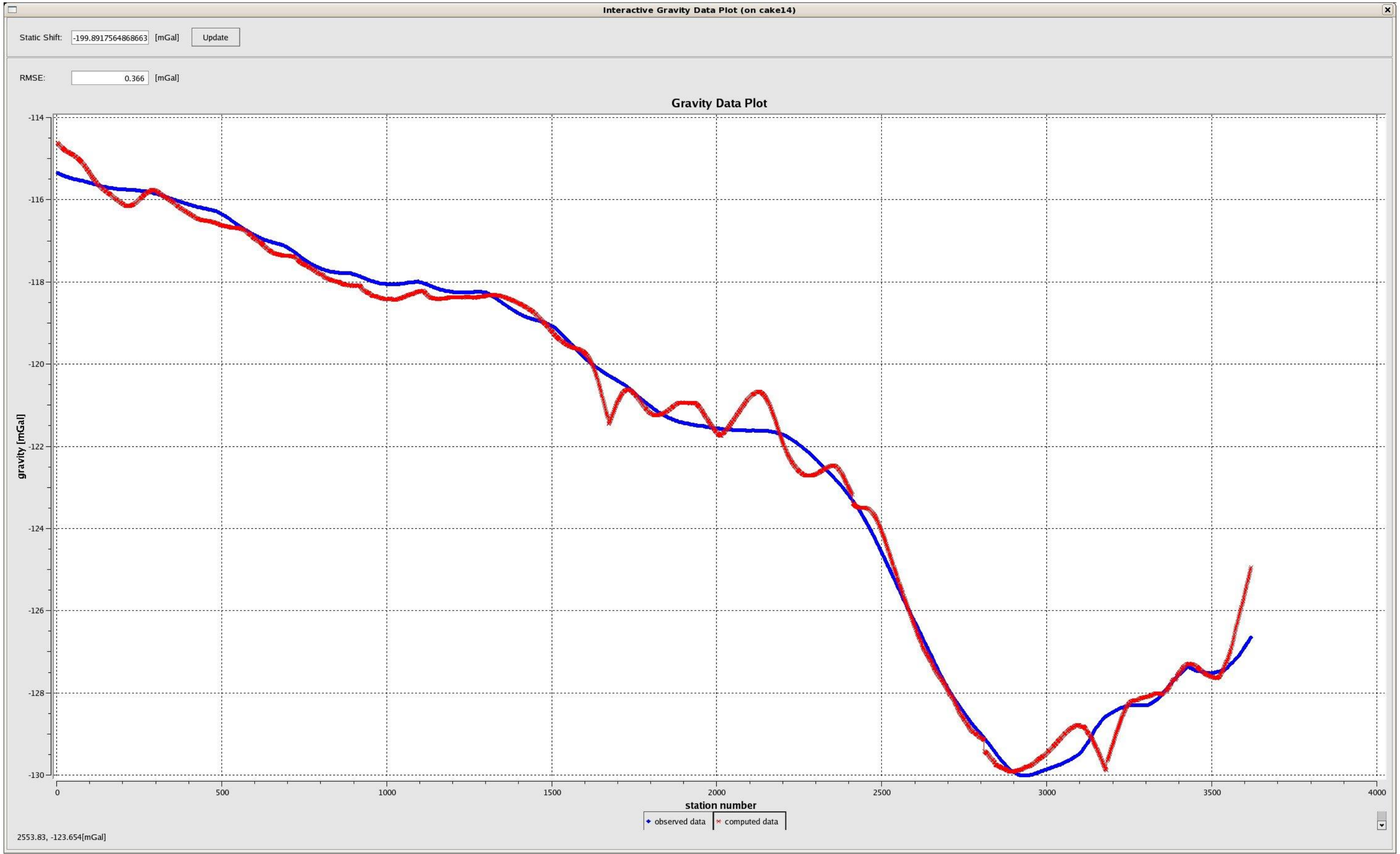

Figure 20 Line 05: Bouguer anomaly fit of the last inverted model.

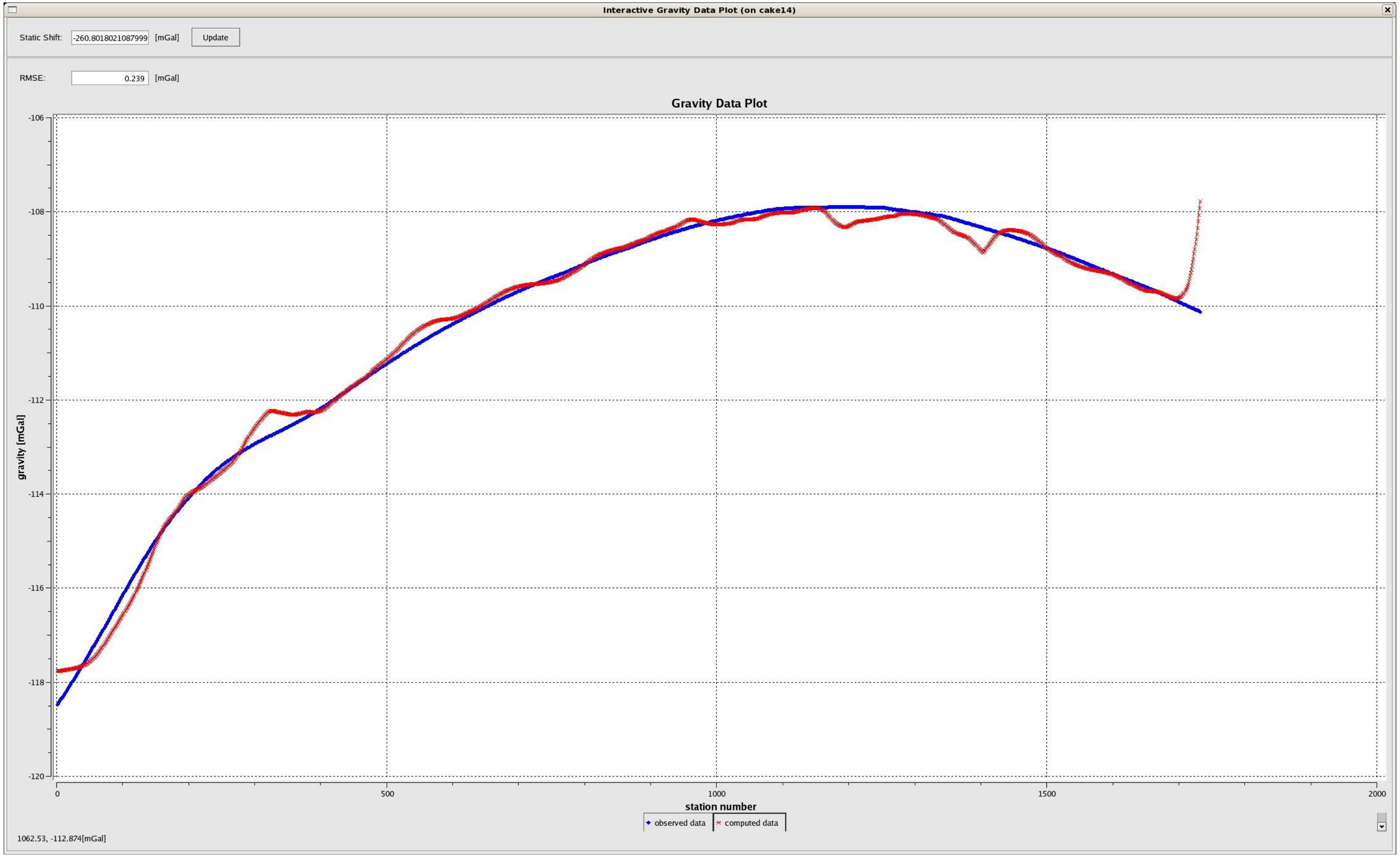

Figure 21 Line 10: Bouguer anomaly fit of the last inverted model.

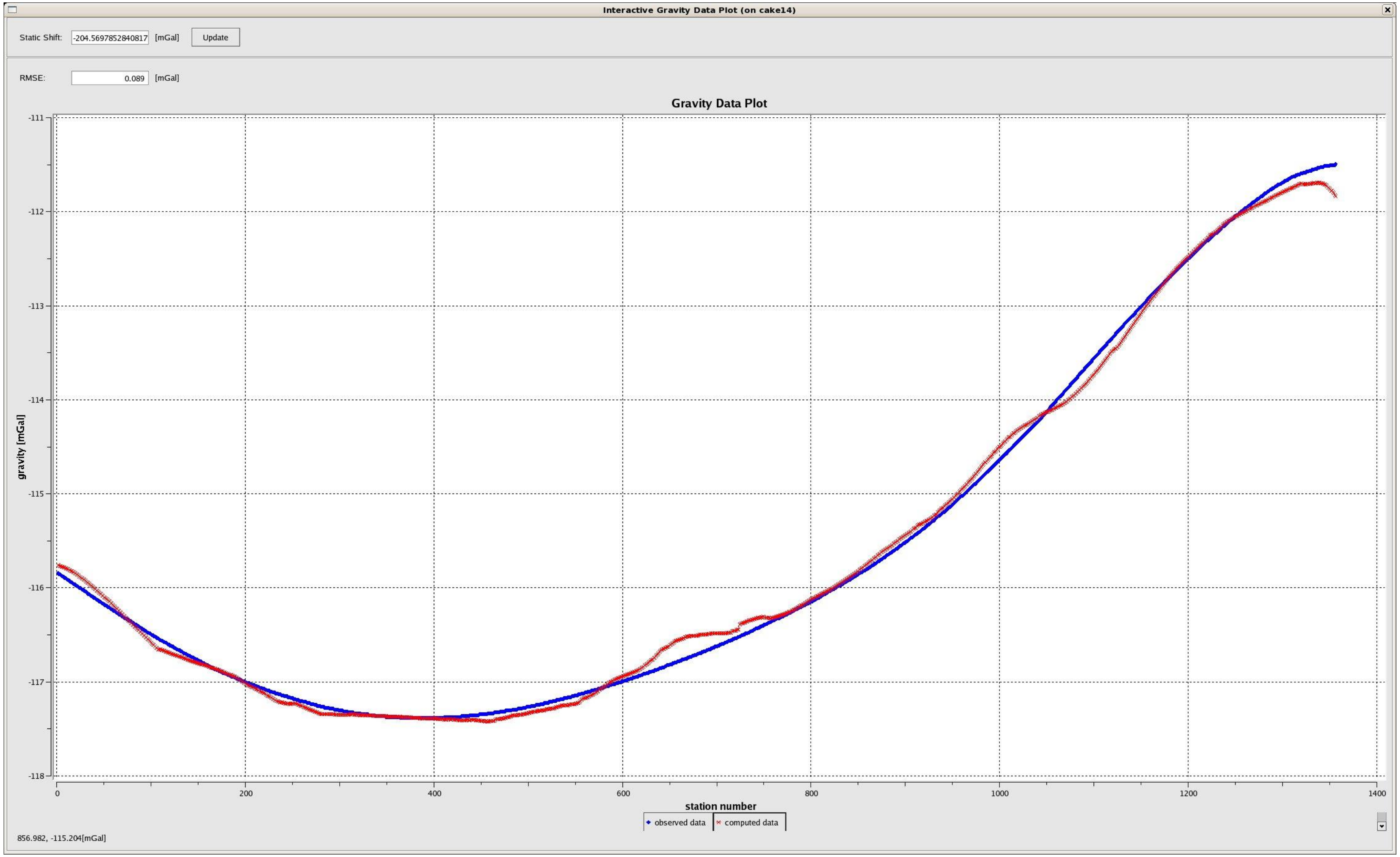

Figure 22 Line 15: Bouguer anomaly fit of the last inverted model

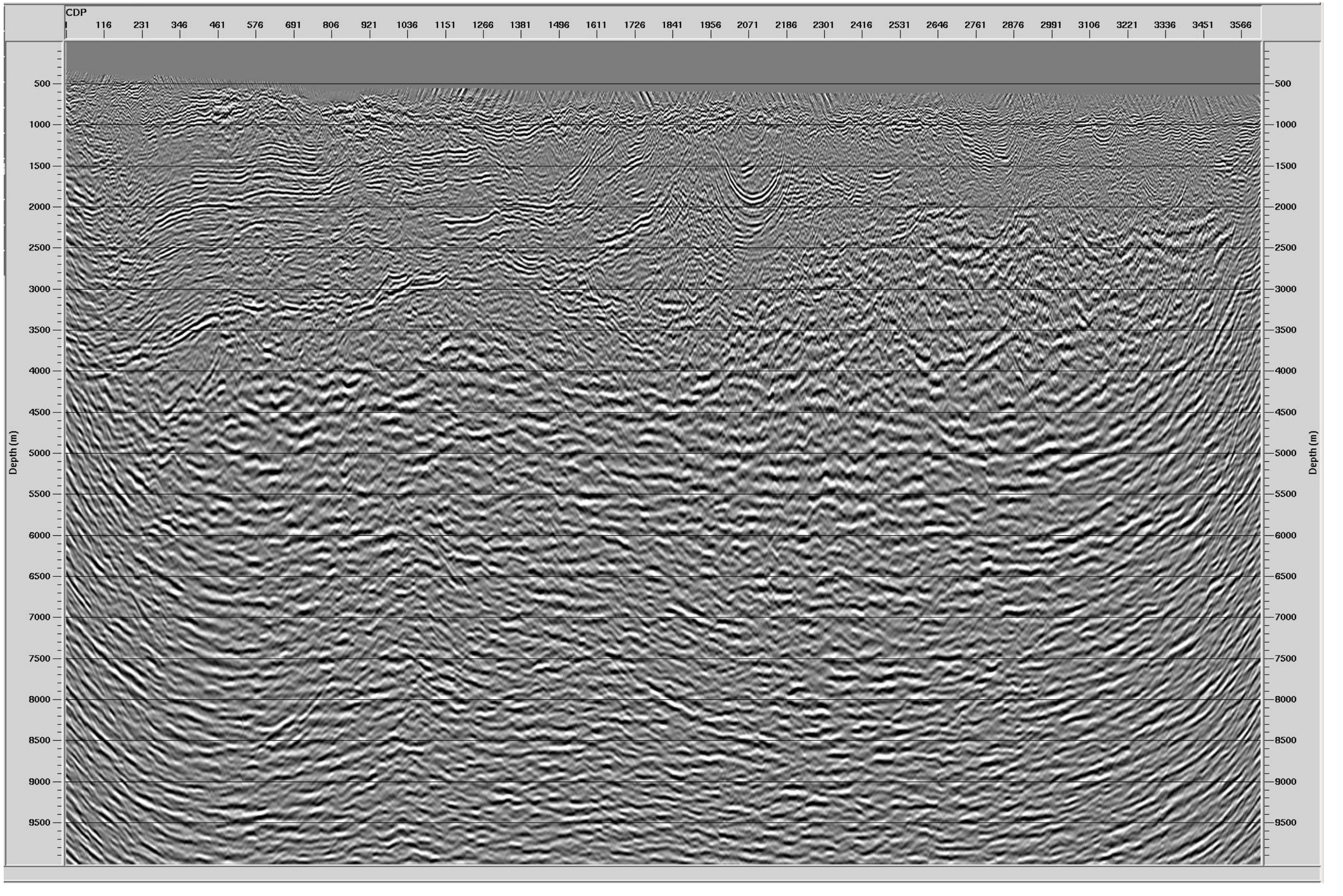

Figure 23 Line 05: final depth section from PSDM processing

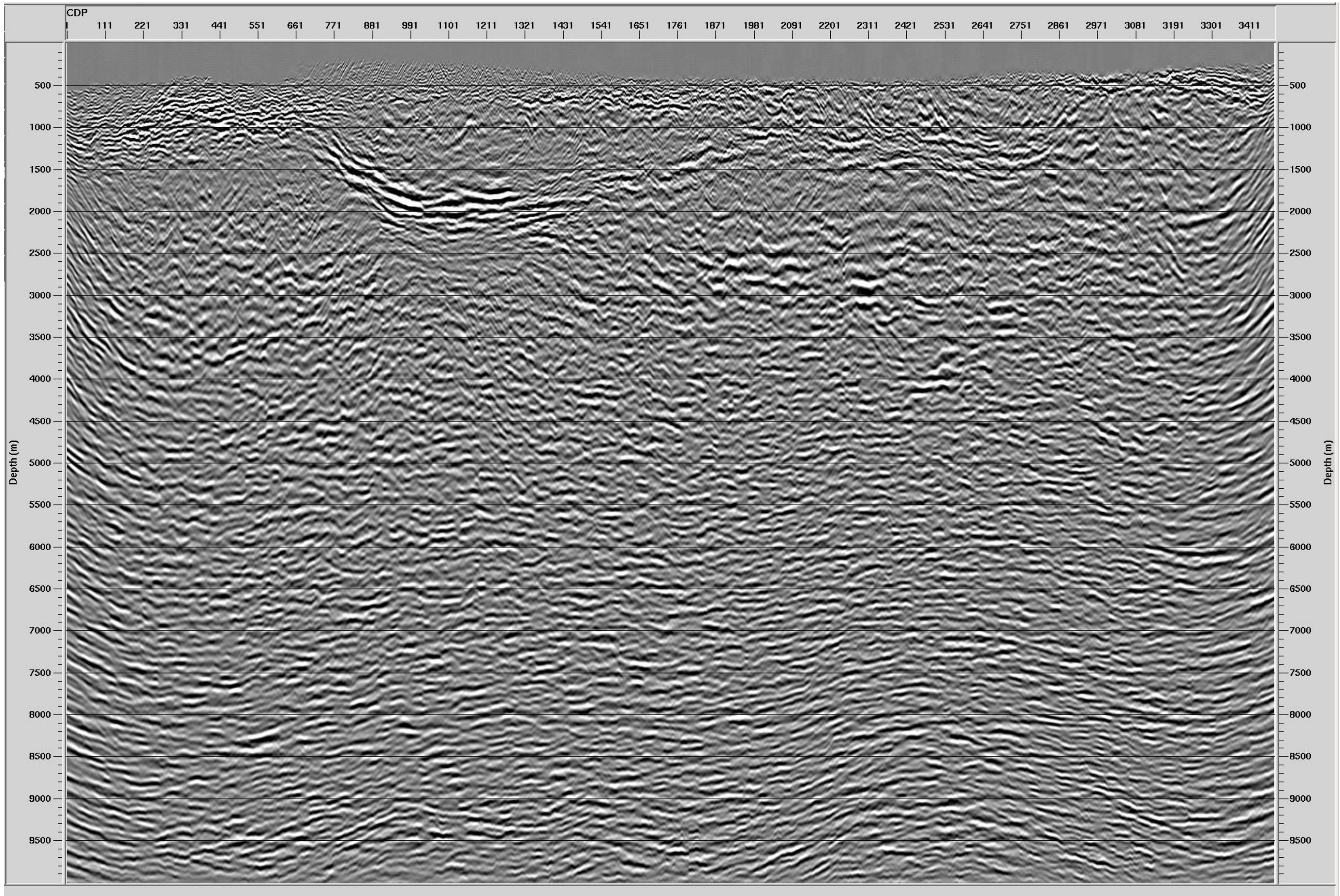

Figure 24 Line 10: final depth section from PSDM processing

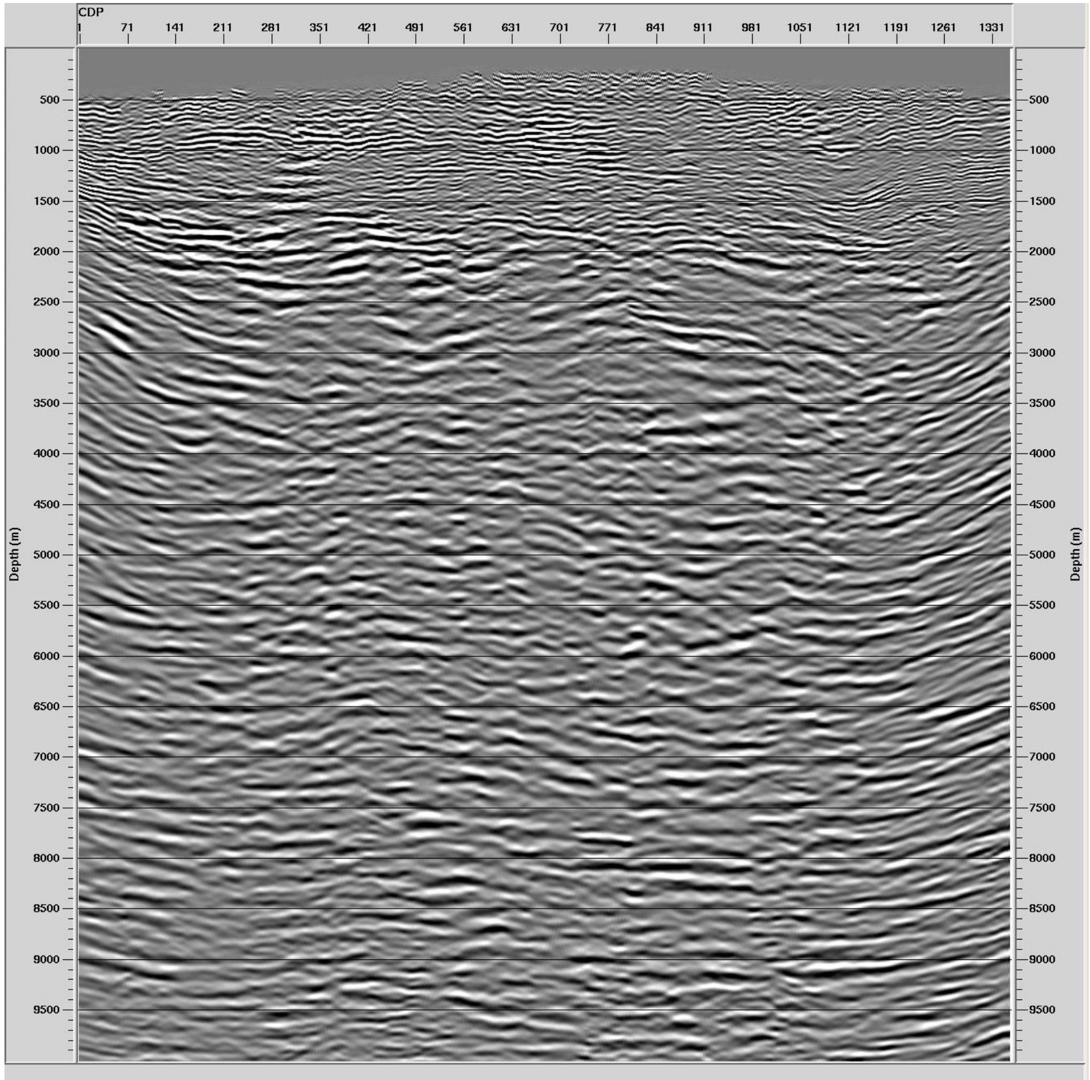

Figure 25 Line 15: final depth section from PSDM processing

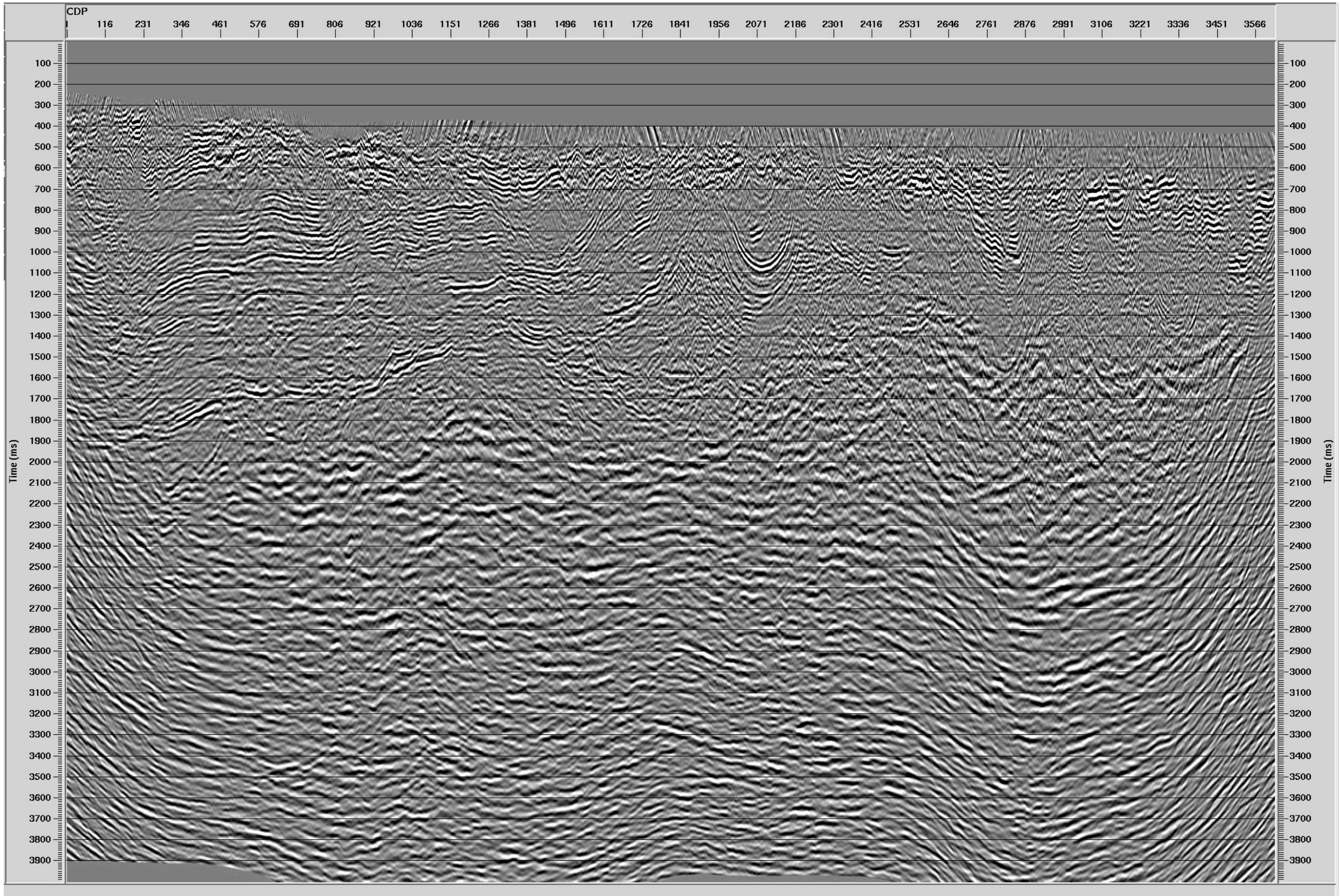

Figure 26 Line 05: time-stretched PSDM.

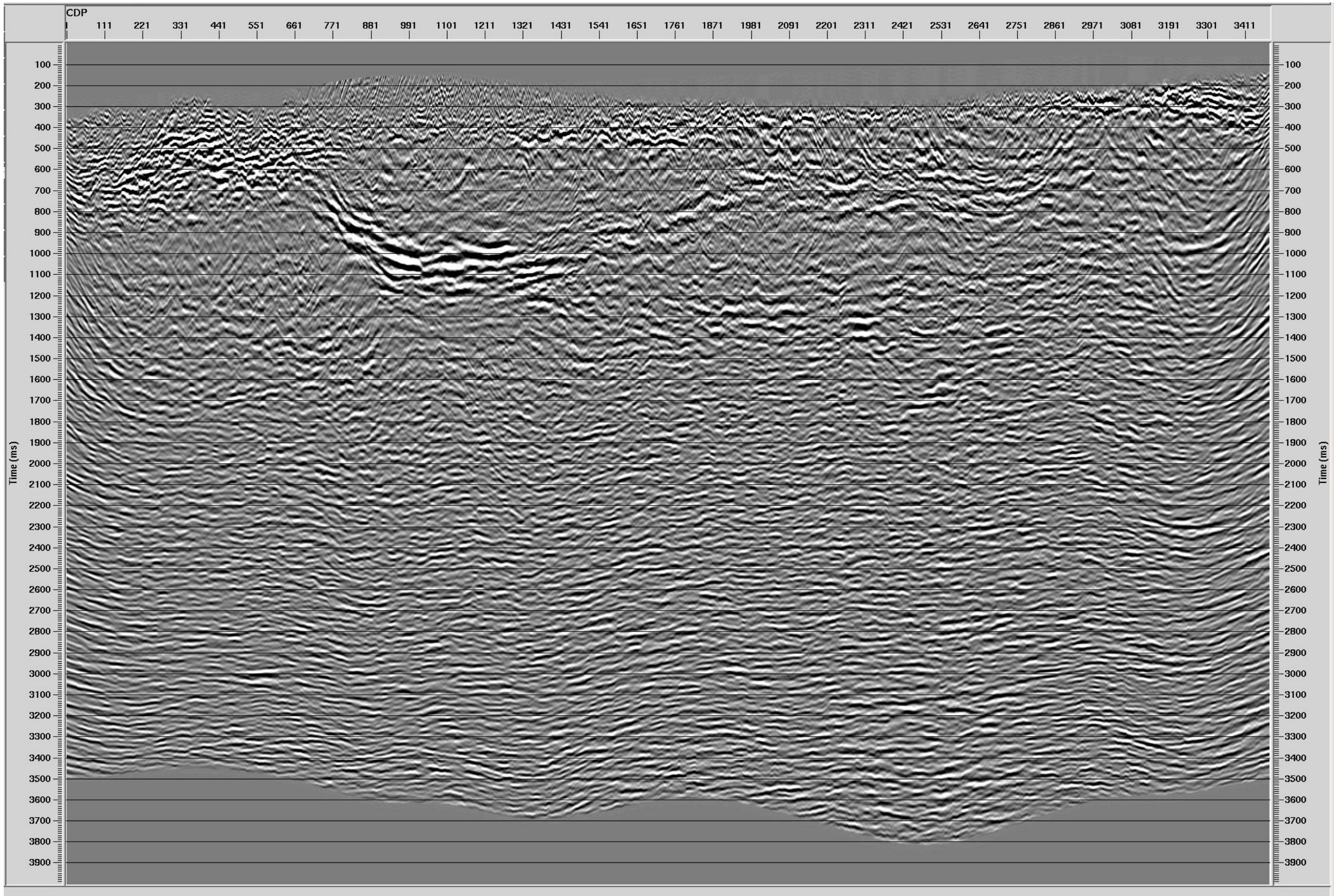

Figure 27 Line 10: time-stretched PSDM.

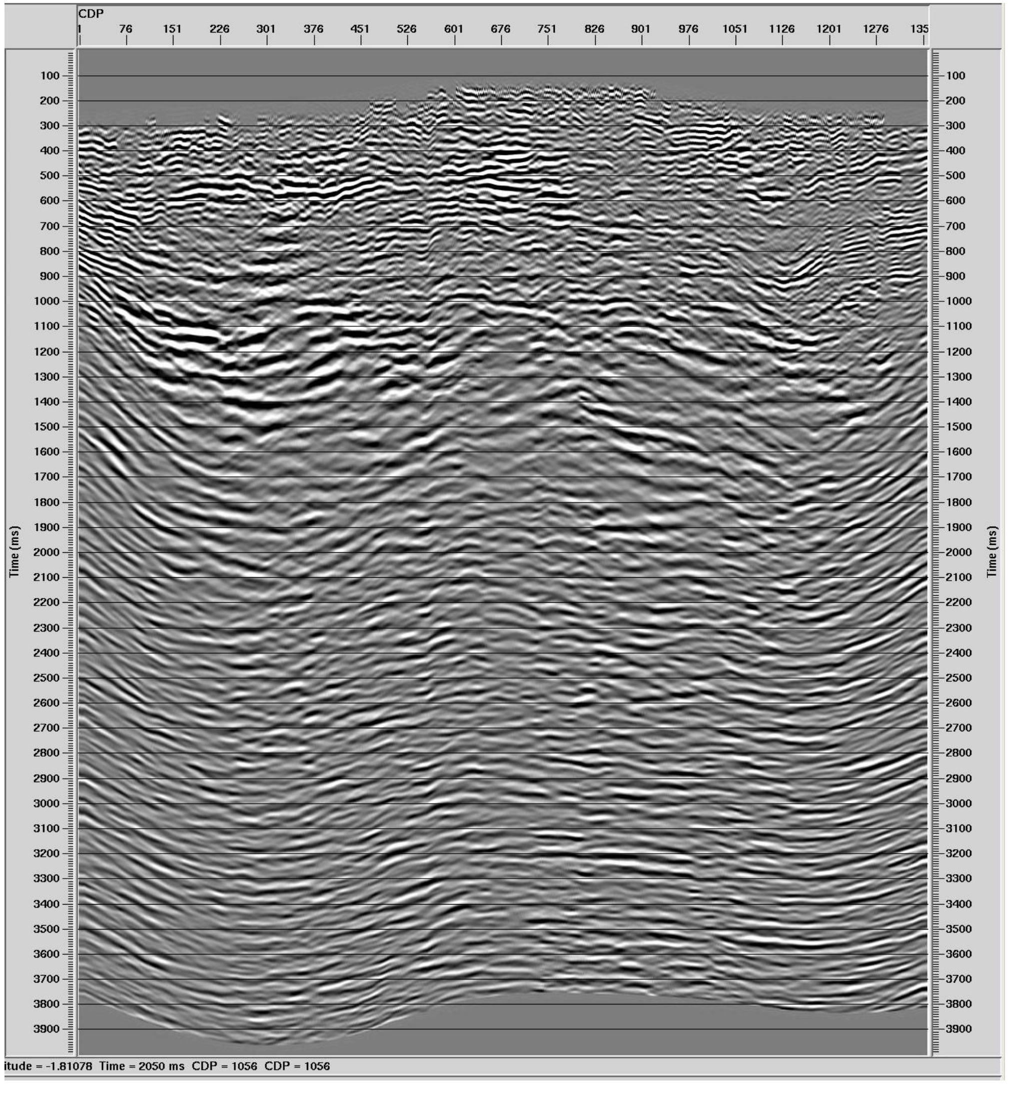

Figure 28 Line 15: time-stretched PSDM.

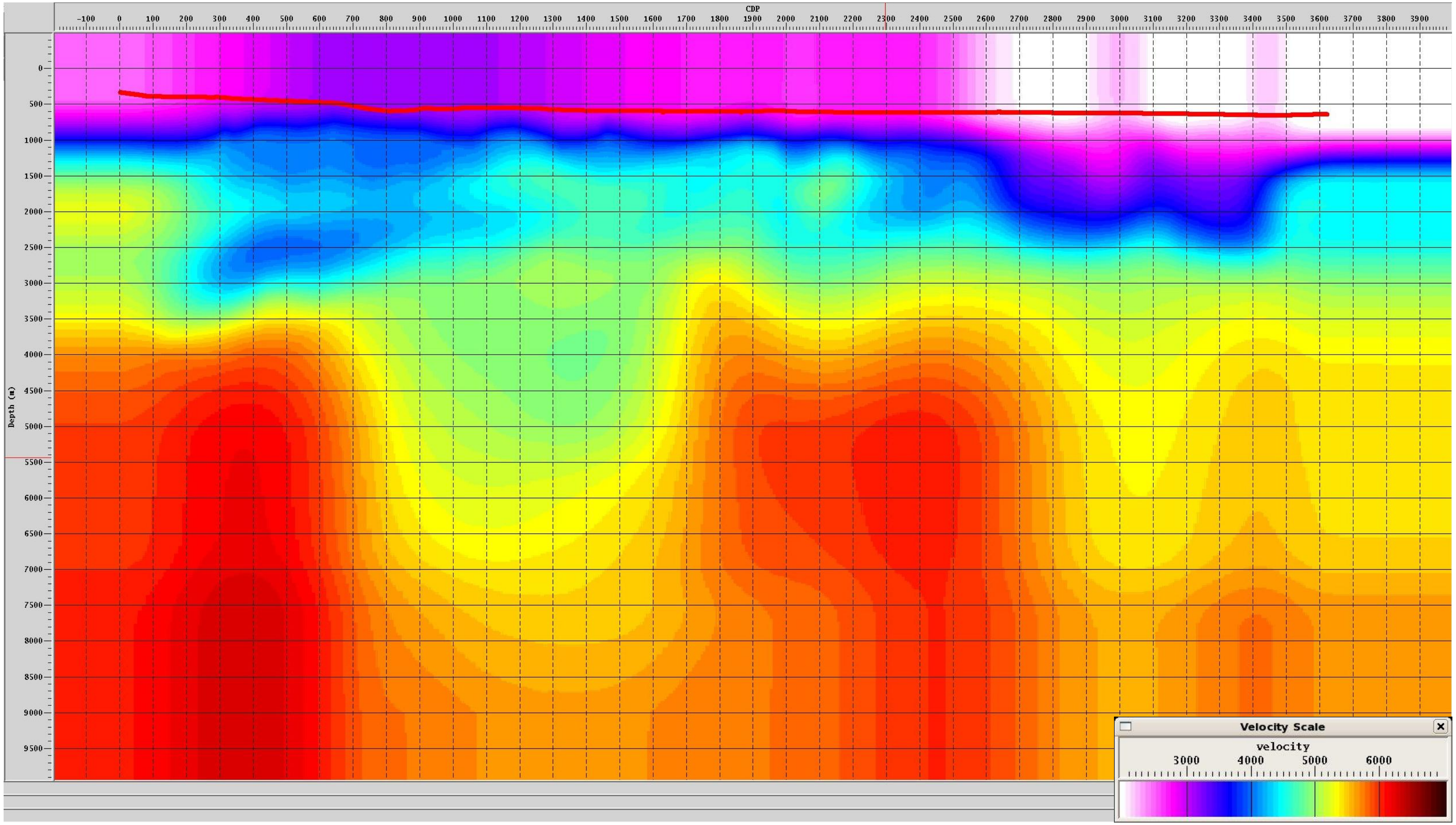

Figure 29 Line 05: final velocity model.

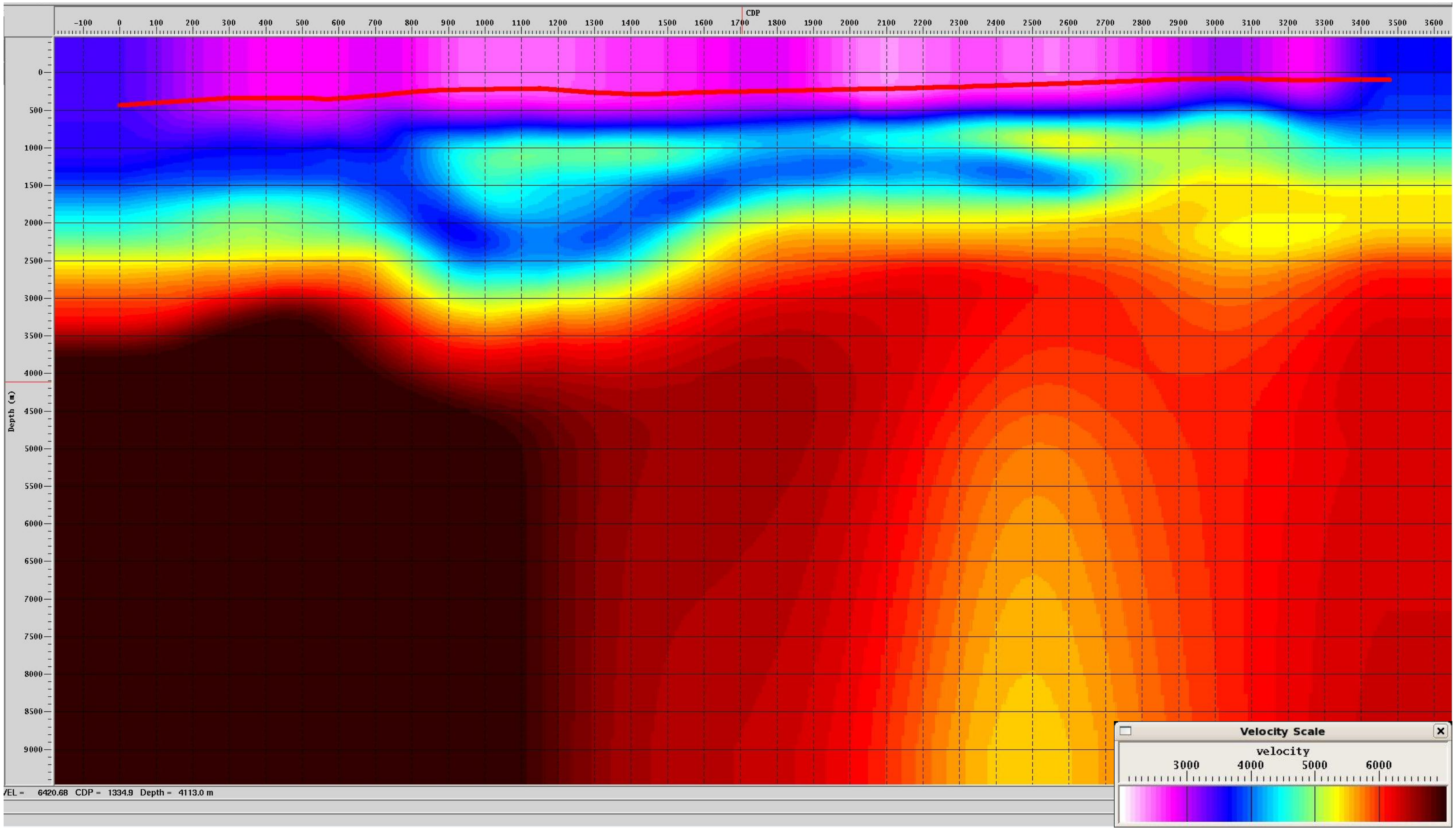

Figure 30 Line 10: final velocity model.

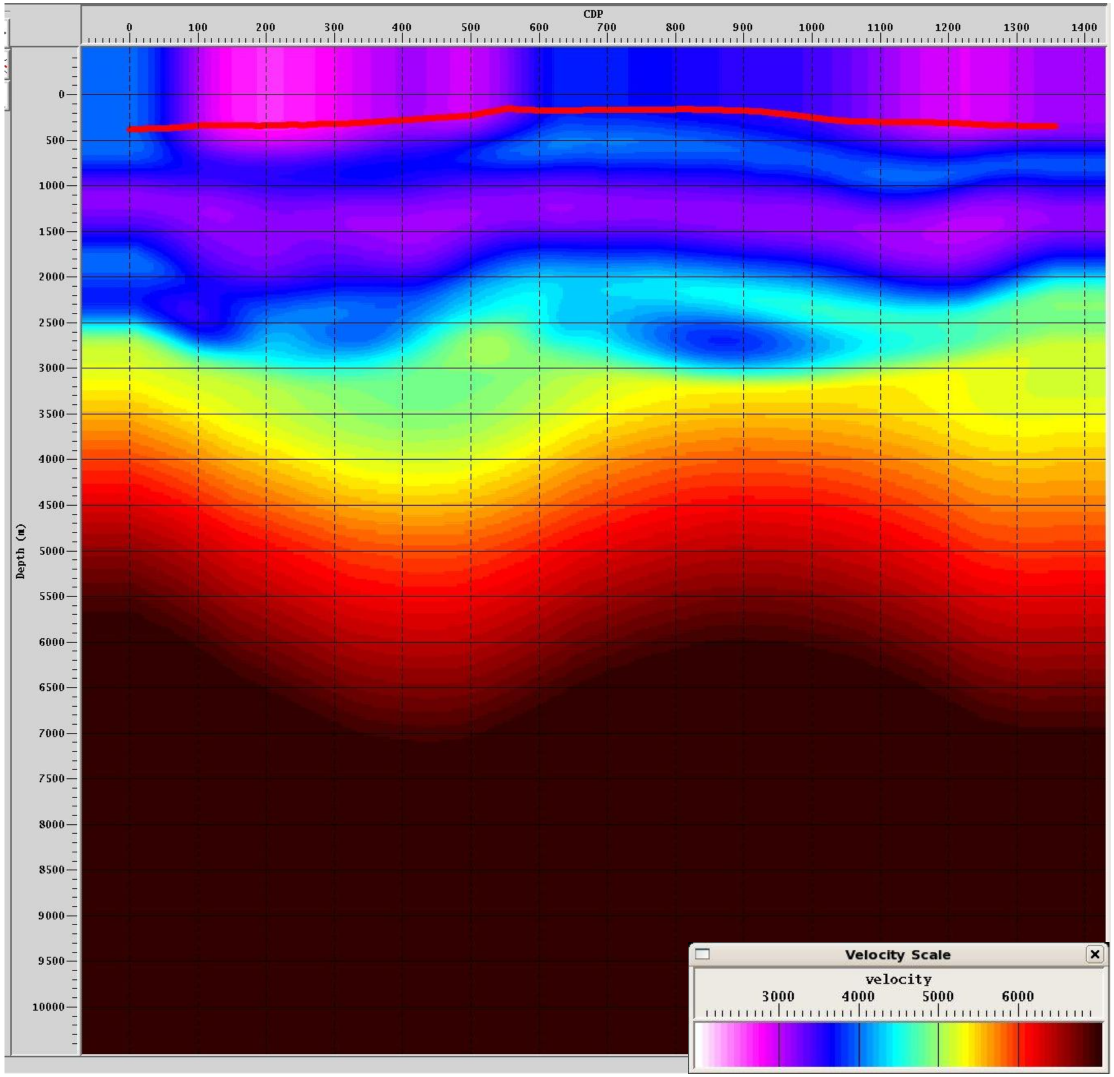

Figure 31 Line 15: final velocity model.

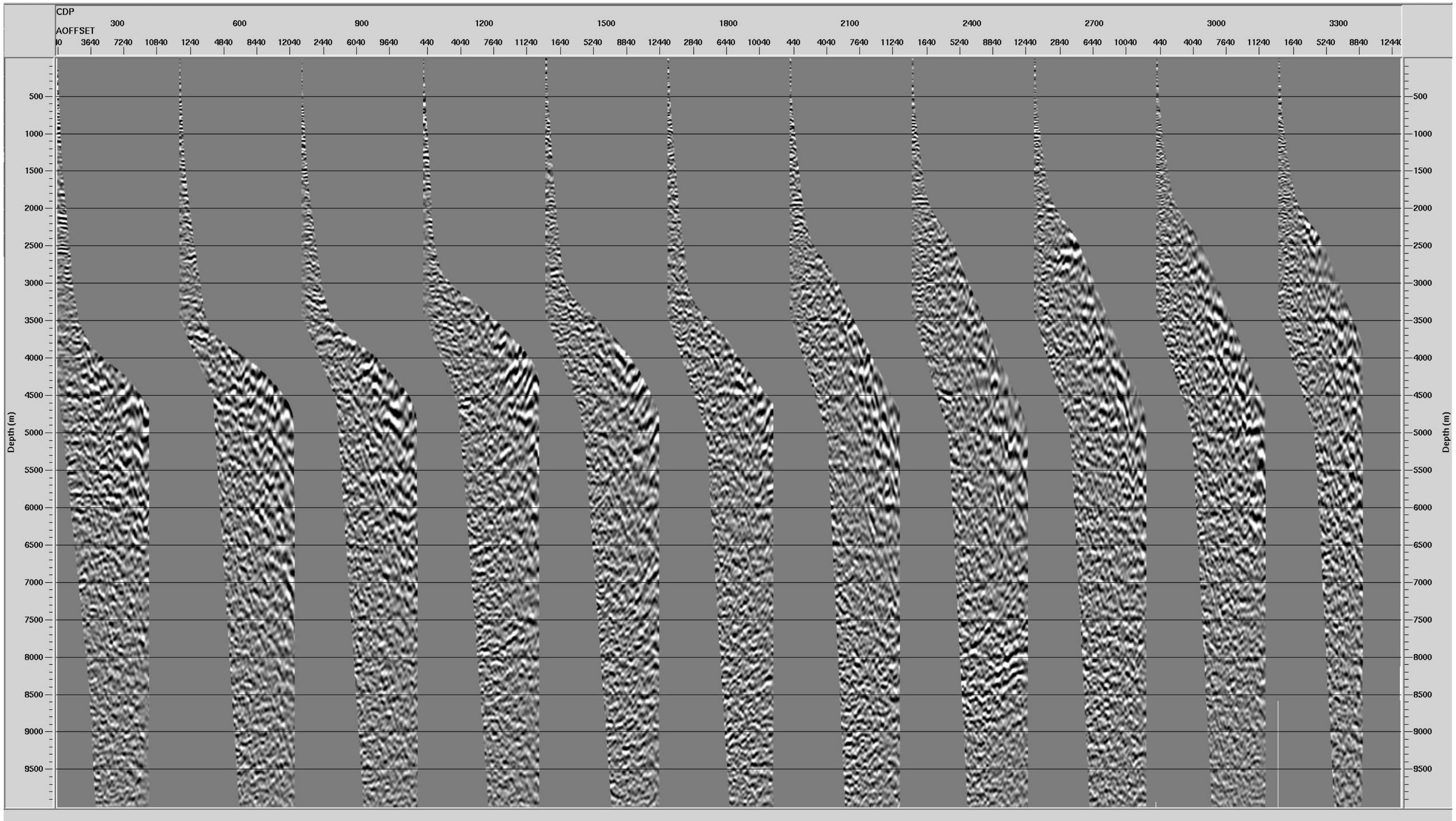

Figure 32 Line 05: final PSDM common image gathers

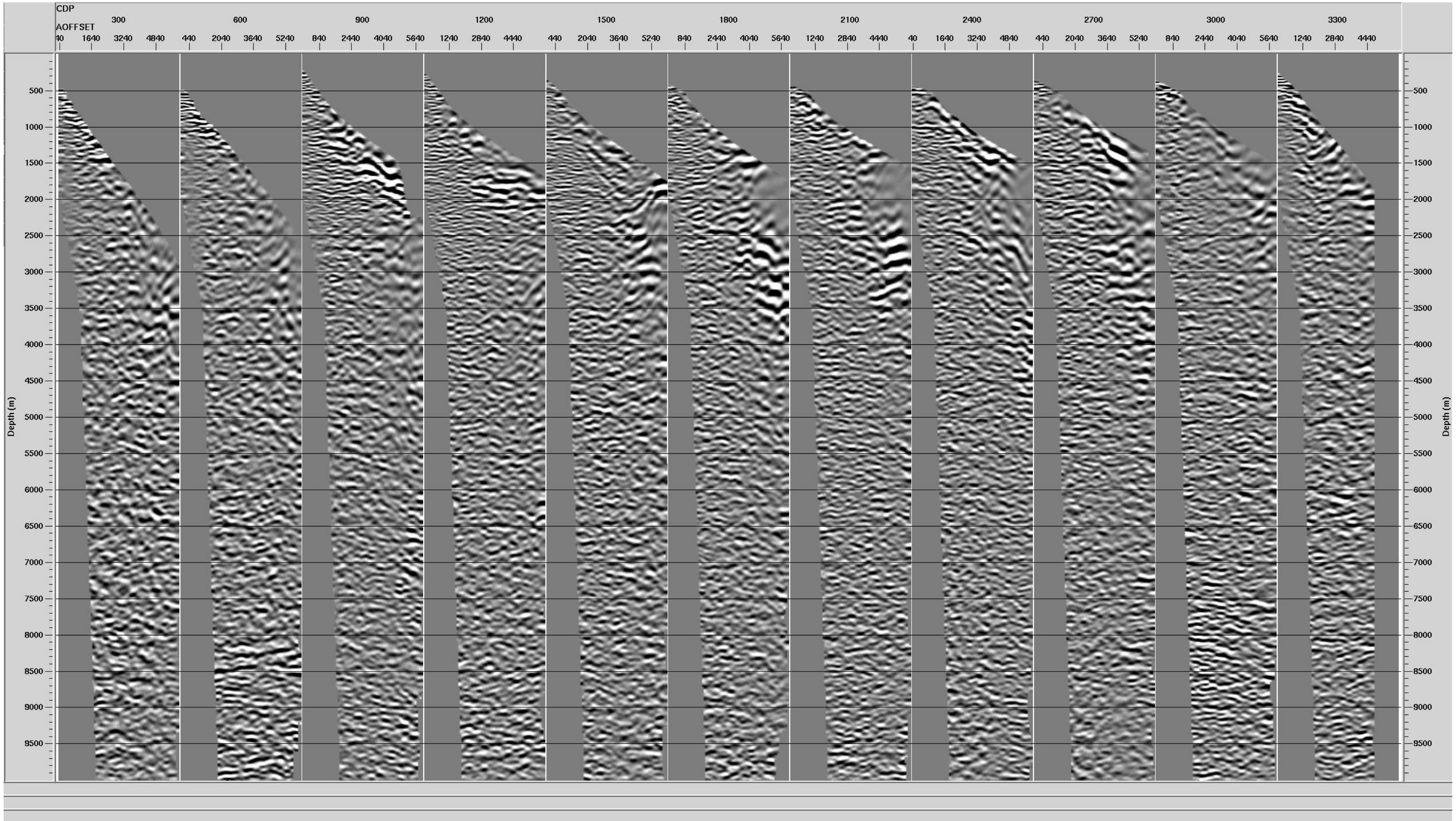

Figure 33 Line10: final PSDM common image gathers

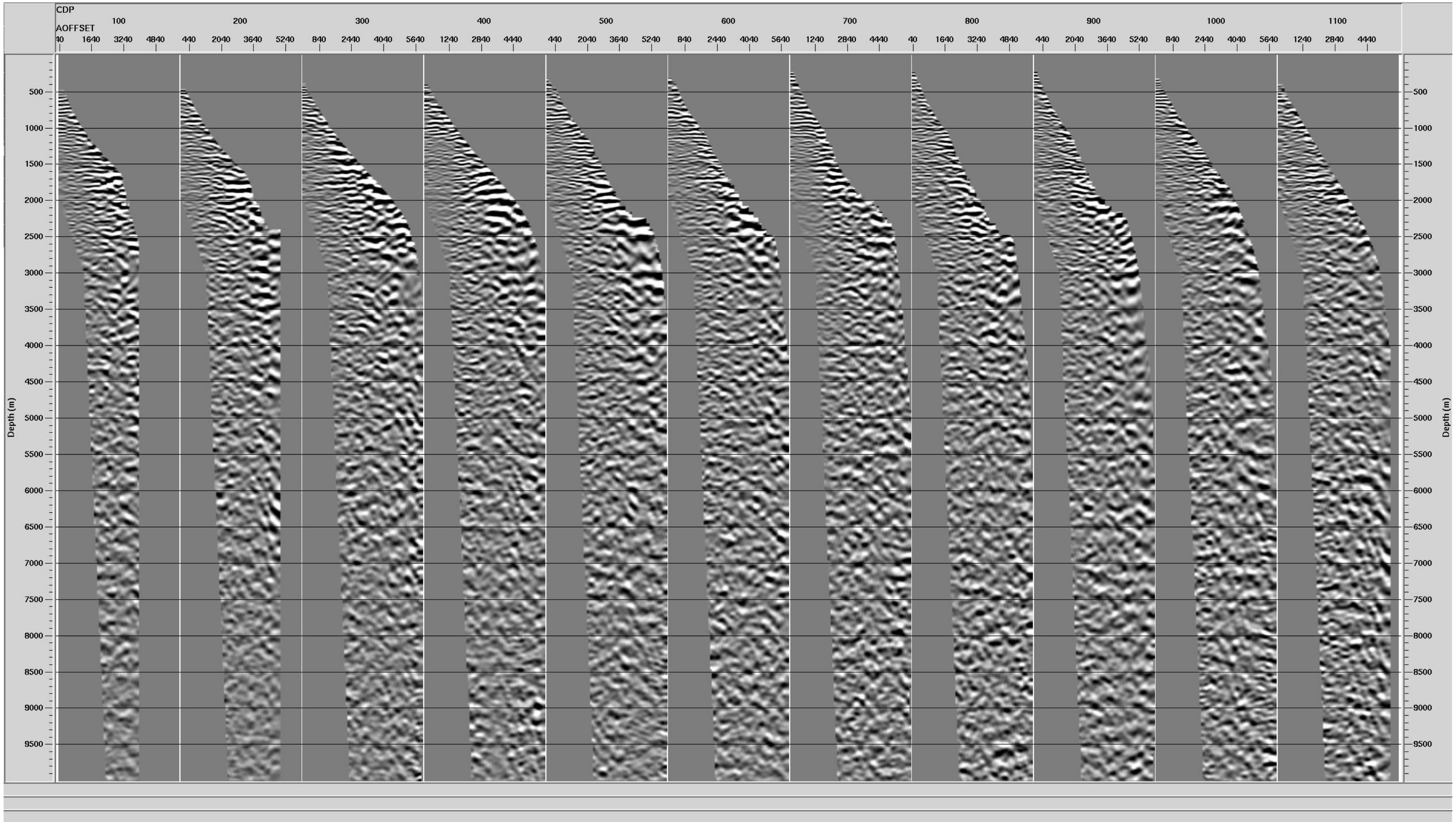

Figure 34 Line 15: final PSDM common image gathers